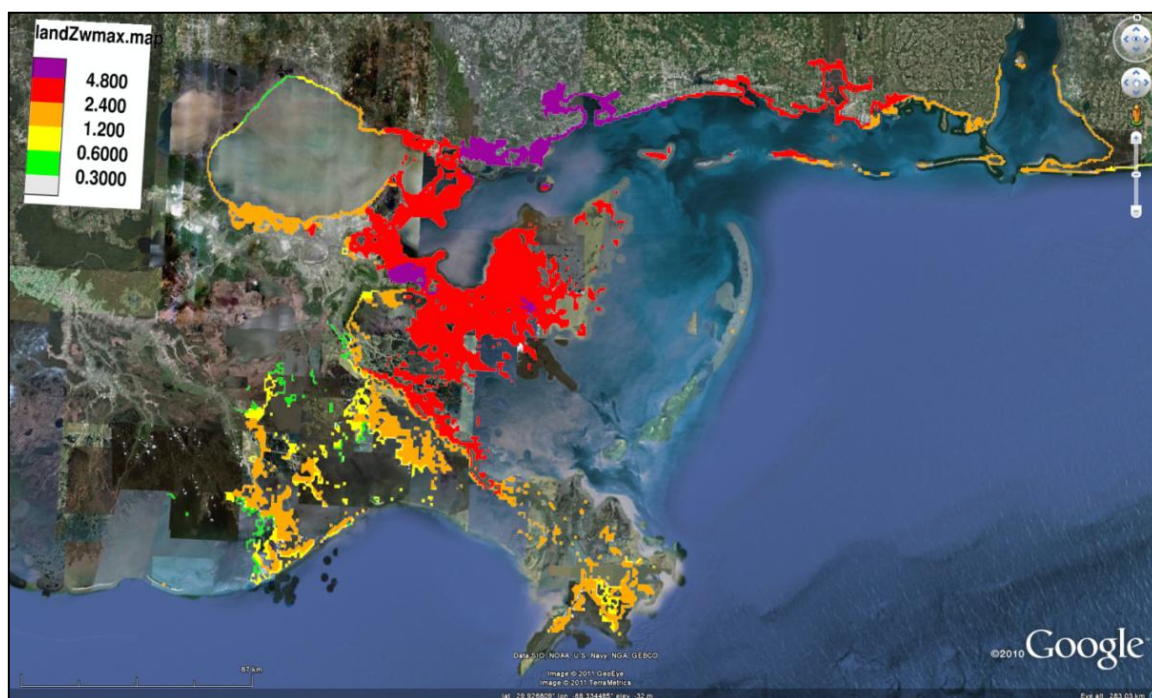


Global storm surge forecast and inundation modeling

Pamela Probst
Giovanni Franchello

Joint Research Centre, European Commission



The mission of the JRC-IPSC is to provide research results and to support EU policy-makers in their effort towards global security and towards protection of European citizens from accidents, deliberate attacks, fraud and illegal actions against EU policies.

European Commission
Joint Research Centre
Institute for the Protection and Security of the Citizen

Contact information: Giovanni Franchello

Address: JRC Ispra Site, Via Enrico Fermi 2749, I-21027 Ispra (VA), Italy

E-mail: giovanni.franchello@jrc.ec.europa.eu

Tel.: +39 0332 785066

Fax: +39 0332 785154

<http://ipsc.jrc.ec.europa.eu/>

<http://www.jrc.ec.europa.eu/>

Legal Notice

Neither the European Commission nor any person acting on behalf of the Commission is responsible for the use which might be made of this publication.

***Europe Direct is a service to help you find answers
to your questions about the European Union***

Freephone number (*):

00 800 6 7 8 9 10 11

(*). Certain mobile telephone operators do not allow access to 00 800 numbers or these calls may be billed.

A great deal of additional information on the European Union is available on the Internet. It can be accessed through the Europa server <http://europa.eu/>

JRC 68133

EUR 25233 EN

ISBN 978-92-79-23176-6

ISSN 1831-9424

DOI 10.2788/14951

Luxembourg: Publications Office of the European Union, 2012

© European Union, 2012

Reproduction is authorized provided the source is acknowledged

Printed in Italy

ABSTRACT

Tropical cyclones (TCs) are some of the most damaging events. They occur in yearly cycles and affect the coastal population with three dangerous effects: heavy rain, strong wind and storm surge. In order to estimate the area and the population affected by a cyclone, all the three types of physical impacts must be taken into account. Storm surge is an abnormal rise of water above the astronomical tides, generated by strong winds and drop in the atmospheric pressure. The report describes the implementation of such phenomena in the JRC HyFlux2 code, which is routinely used in GDACS (www.gdacs.org) to model inundations due to tsunami run-ups.

The first aim of this work is to identify which source of information (provided by the different weather forecast centers) allows the specification of the pressure and wind fields of the TCs at global level. The lack of a global and free downloadable TC wind and pressure datasets has led the JRC to develop a Monte Carlo method to determine the Holland's parameters using the world available wind radii data (advisory and forecast). The obtained Holland's parameters are therefore used to obtain pressure and wind fields which are the forcing of the HyFlux2 storm surge modeling.

The developed methodology has been validated for four TCs: Earl, Nargis, Katrina and Yasi. The preliminary results show that it is possible to forecast the effects of storm surges by several days in advance.

CONTENTS

1. INTRODUCTION
2. STORM SURGE MODELING
 - 2.1. Stat-of-the-art of storm surge codes
 - 2.2. Hyflux2 code for inundation modeling
3. ATMOSPHERIC FORCING
 - 3.1. Data Sources
 - 3.1.1 Forecasting products
 - 3.1.2 Post-analysis products
 - 3.1.3 Atmospheric data set comparisons and discussion
 - 3.2. Holland's parametric model
 - 3.3. Wind radii treatment
4. STORM SURGE SIMULATIONS
 - 4.1. KATRINA
 - 4.2. NARGIS
 - 4.3. YASI
5. CONCLUSIONS
6. REFERENCES

APPENDICES

- A. Tropical Warning Centers
- B. Saffir-Simpson Scale

1. INTRODUCTION

The Joint Research Centre (JRC) of the European Commission has developed the Global Disasters Alert and Coordination System (GDACS, www.gdacs.org), an early warning system created to alert the humanitarian community about potential disasters which are under development. The system automatically invokes ad hoc numerical models in order to analyze the level of the hazard of natural disasters like earthquakes, tsunamis, cyclones, floods, volcanoes. Tropical cyclones (TCs) are some of the most damaging events. They occur in yearly cycles and affect the coastal population with three dangerous effects: heavy rain, strong wind and storm surge. In order to estimate the area and the population affected by a cyclone, all the three types of physical impacts must be taken into account. Therefore JRC is implementing the storm surge phenomena in the HyFlux2 code (Section 2), routinely used in GDACS to model inundation due to tsunami run-ups.

In storm surge modeling, various physical processes have to be taken into account, such as Coriolis Forces, Bottom Friction, Pressure Drop, Wind Friction, Radiation Stress and Tides. Storm surge is an abnormal rise of water above the predicted astronomical tides, generated by strong winds and drop in the atmospheric pressure. Therefore, the primary forcing term is the atmospheric forcing: wind friction and pressure gradient. Actual and forecasted surface wind and atmospheric pressure fields, defined in the entire computational space domain are required for the hydrodynamic HyFlux2 simulations.

The first aim of this work is to identify which source of information (provided by the different weather forecast center) allows the specification of the pressure and wind field of the TCs at global level.

The real-time data of wind and surface pressure are insufficient to allow a direct analysis of the central region of most TCs and they cannot be used alone to generate the wind field needed for a storm surge model (Powell et al., 2010). For this reason several models have been developed to infer wind and pressure fields. An overview on the main approaches used in TC wind field modeling is presented in Harper et al. (2001) and in Cardone et al. (2009). In particular Cardone et al. (2009) explore the sensitivity of predictions of coastal surges to wind fields developed by alternative methods, presenting interesting results and a discussion of sources of uncertainties of the different wind analysis methods. In this article the main approaches used in TC wind field modeling are described and categorized as: 1) Simple analytical parametric models, such as Holland's model (Holland, 1980); 2) steady-state dynamical model, such as PBL model (Chow, 1970; Cardone et al., 1976; Shapiro, 1983; Thompson, et al., 1996; Vickery et al., 2000); 3) Non-steady dynamical models such as Geophysical Fluid Dynamics Laboratory (GFDL) (Kurihara et al., 1998); 4) kinematical methods, such as National Oceanic and Atmospheric Administration (NOAA) National Hurricane Research Division H*Wind (Powell et al., 1996) and Oceanweather's IOKA (Cox et al., 1995).

The widely and well known method suitable to specify pressure and wind fields is the Holland's parametric model (Holland, 1980), which contains some parameters empirically estimated from observations or determined climatologically. This model is widely used in risk assessment (Vickery et al., 2009). The Holland's model is axis-symmetric, therefore several considerations and additional terms must be included in order to consider the asymmetry of the real fields (Harper et al., 2001). Moreover this model needs several input parameters (hereafter called Holland's parameters), such as the TC track, mean sea level pressure of TC center (P_c), radius of maximum wind (R_{max}) and maximum wind velocity (V_{max}). These parameters unfortunately are not always available globally. Every 6-hours the TC warning centers (Appendix A) publish a TC bulletin, including information such as wind speed, pressure, and track locations which are used as input for the parametric model (e.g. Holland's model), but these information are not available in each TC basin (Knaff et al., 2010). Several methods have been developed to infer the missing parameters, such as the wind-pressure relationship (Atkinson et al., 1977; Courtney et al., 2009). Unfortunately all these relations are based on datasets of varying quality and with a lack of suitable observational data that makes validation difficult (Knaff et al., 2010).

TC products suitable to infer the pressure and wind fields are available from several weather forecasting centers such as the GFDL and European Centre for Medium-Range Weather Forecasts (ECMWF) TC products. Unfortunately some TCs products are not available globally or are not available in real time.

Another way to infer the pressure and wind field is to use the global forecasting model such as the Global Forecasting System (GFS) model (Hamill et al., 2011). In the past the global models, due to the coarse grid size (around 55 Km), had several problems to resolve the extreme pressure gradients associated with TCs (Van Der Grijin, 2002), but in 2010 the NOAA and ECMWF global models have improved notably their resolution. Actually the NOAA GFS model has a resolution of 27 km, while that of ECMWF has a resolution of 16 km. These recent improvements on the global resolution, should be able to reproduce the extreme pressure gradient inside a TC, as shown in Miller (2010).

In the past decade, a new TC parameter has been made available in the TC bulletins data source: the wind radii. This term represents the maximum radial extent – in nautical miles - of winds reaching 34, 50, and 64 knots in each quadrant (NE, SE, SW, and NW). These data are provided in each TC bulletin issued by the TC warning centers at least every six hours. A method based on the Holland's model which uses these data as input

represents another possibility to infer the wind and pressure fields as shown in Xie et al. (2006). They developed a real-time TC wind forecast system by incorporating the asymmetric representation of a TC wind field into the Holland's model. To provide optimized asymmetric hurricane wind forecasts, the National Data Buoy Center (NDBC) real-time buoy data have been introduced into the model's initial wind field and the NOAA National Hurricane Center's (NHC) TC bulletin information (Track, P_c , V_{max} and wind radii data), are used for prognostic modeling. This method has been validated for the Atlantic basin, reaching interesting results. This method required as input also P_c , but this parameter is not available in each TC basin.

The lack of a global and free downloadable dataset of TC wind and pressure datasets has led the JRC to develop a method to determine the Holland's parameters, using the world available wind radii data (advisory and forecast). The developed method that will be described in the report is validated for four TCs: Earl, Nargis, Katrina and Yasi. Earl was a strong TC that affected most of the United States east coast and Canada (25 August- 3 September 2010). Nargis was a strong TC that caused the worst disaster in the history of Myanmar (27 April – 3 May 2008). Katrina was one of the most damaging TCs disasters in the history of the United States (23 – 30 August 2005). Yasi was an intense TC that caused significant damage to Queensland, Australia (30 January – 3 February 2011). The Holland's parameters obtained from the wind radii are then used to obtain pressure and wind fields which are the forcing of the HyFlux2 storm surge modeling of the last three TCs.

An overview on storm surge modeling and the basic characteristics of the HyFlux2 model used at JRC are presented in Section 2, while the Holland's model and the JRC method developed to determine the Holland's parameter using the wind radii are presented in Section 3. A preliminary result of storm surge using the developed methods is shown in Section 4. Concluding remarks are in Section 5.

2. STORM SURGE MODELING

2.1. State of the art of storm surge codes

Storm surge is an abnormal rise of water generated by a storm above the predicted astronomical tides, generated by strong winds and by a drop in the atmospheric pressure. These meteorological phenomena constitute the atmospheric forcing and will be described in Section 3.

These effects generate long waves, called storm surges, with a characteristic time-scale of several hours to one day and a wavelength approximately equal to the width of the center of the depression typically between 150 and 800 km (CIRIA et al., 2007). Therefore these long waves can be represented by the shallow water equations (Eq.1).

In addition to pressure drop and wind friction, a storm surge model can include also others physical processes such as Coriolis Forces, Bottom Friction, Radiation Stress and Tides.

A wide range of storm surge models are used for predicting the TC impact. A complete state-of-the-art of the storm surge models with their main characteristics are in Harper et al. (2001) and in Dube et al. (2010), while in Alimov (2005) several models are described in detail, showing their limits and advantage in their usage. In next Section the JRC code HyFlux2 is presented, while below the following three models are presented: the Sea, Lake and Overland Surges from Hurricanes (SLOSH), the (parallel) ADvanced CIRculation (ADCIRC) Coastal Circulation and Storm Surge Model, and the Japan Meteorological Agency (JMA) storm surge model.

SLOSH is a computer code developed by Federal Emergency Management Agency (FEMA), United States Army Corps of Engineers and by the National Weather Service to define flood-prone areas for evacuation planning. It is run by the NOAA National Hurricane Centre to estimate storm surge heights and winds resulting from historical, hypothetical, or predicted hurricanes. SLOSH model solves the depth-integrated shallow water equations using a finite difference solution and a polar or elliptical/hyperbolic grid type (depending on the specific coastal area called basin). The model includes the astronomical tides, specifying an initial tide level. It does not include rainfall amounts, riverflow, or wind-driven waves. The covered areas are: U.S. East Coast, Gulf of Mexico, parts of Hawaii, Guam, Puerto Rico, Virgin Islands, Various basins in China and India. More information can be found in Jelesnianski et al. (1992), Glahn et al. (2009), Dube et al. (2010), on the NOAA NHC website (<http://www.nhc.noaa.gov/HAW2/english/surge/slosh.shtml>) and FEMA website (<http://www.fema.gov/hazard/hurricane/index.shtm>).

ADCIRC, developed by Leuttich, et al. (1992) is a computer code that computes surface water elevation and currents. It solves the depth-integrated shallow-water equations using a finite-element solution and an unstructured grid. The model domain extended across the Gulf of Mexico and Caribbean Sea to an open boundary in the mid-Atlantic. More information can be found in Blain et al. (1994) and in Leuttich et al. (1992) and at <http://www.adcirc.org/>.

SLOSH and ADCIRC have different approaches and therefore they have a different strengths and weakness (Alimov, 2005). SLOSH model has lower run-time than ADCIRC, but the resolution of ADCIRC is

much higher. Therefore these models are suitable for different situations, despite sometime they are used for similar task. These models are used in the following studies: Cardone et al. (2009), Melton et al. (2009), Niedoroda et al. (2010), Dietrich et al. (2010) and Bunya et al. (2010).

JMA storm surge model solves the two-dimensional shallow water equations using a finite difference method. This model includes the atmospheric forcing (described in Section 3) using two different methods to allow the uncertainty in TC track forecasts; the parametric model (Fujita, 1952) and the operational non-hydrostatic model (Saito et al., 2006). JMA has also developed a method to include the atmospheric tide effects, developing a data assimilation system to combine the information from observation data and ocean tide model. More information are in Higaki et al. (2008) and Higaki et al. (2009).

2.2. HyFlux2 code for inundation modeling

In the last years JRC has developed extensive experience in tsunami early warning systems, using the JRC-SWAN finite difference code for wave propagation modeling and the JRC finite-volume HyFlux2 code for wave propagation and inundation modeling. Recently, the atmospheric forcing has been included in the HyFlux2 code in order to use it also for storm surge modeling.

HyFlux2 model solves the shallow water equations using a finite volume method. The interface flux is computed by a Flux Vector Splitting method for shallow water equations based on a Godunov-type approach. A second-order scheme is applied to the water surface level and velocity, providing results with high accuracy and assuring the balance between fluxes and sources also for complex bathymetry and topography. Physical models are included to deal with bottom steps and shorelines. The second-order scheme together with the shoreline-tracking method and the implicit source term treatment makes the model well balanced in respect to mass and momentum conservation laws, providing reliable and robust results. More information on the physical models and on the adopted numerical scheme can be found in Franchello (2008), Franchello (2010), Franchello et al. (2008), Cruz et al. (2011) and Zamora et al. (2011).

At the moment, the HyFlux2 code uses uniform Cartesian grid. More detailed inundation simulations are performed by a nested grid approach¹. Developments are in progress in order to adopt a non uniform gridding method, with finer grid in near-shore shallow waters.

Following the 2D shallow water equation:

$$\frac{\partial \mathbf{U}}{\partial t} + \Delta \mathbf{F} = \mathbf{C} \quad (1)$$

where \mathbf{U} is the conservative vector, \mathbf{F} is the flux vector $\mathbf{F} = \{\mathbf{F}_x, \mathbf{F}_y\}$, and \mathbf{C} is the source vector

$$\mathbf{U} = \begin{Bmatrix} h \\ hv_x \\ hv_y \end{Bmatrix} \quad \mathbf{F}_x = \begin{Bmatrix} hv_x \\ hv_x^2 + gh^2/2 \\ hv_x v_y \end{Bmatrix} \quad \mathbf{F}_y = \begin{Bmatrix} hv_y \\ hv_y v_x \\ hv_y^2 + gh^2/2 \end{Bmatrix}$$

$$\mathbf{C} = \begin{Bmatrix} q \\ hfv_y - gh\left(\frac{\partial z}{\partial x} + S_{fx} + S_{px} - S_{ux}\right) \\ -hfv_x - gh\left(\frac{\partial z}{\partial y} + S_{fy} + S_{py} - S_{uy}\right) \end{Bmatrix}$$

Schematic of coordinate and variables of the shallow water model is shown in Figure 1, where h signifies the water depth, $\mathbf{v} = \{v_x, v_y\}$ is the velocity of the fluid in the $\{x, y\}$ plane, z is the vertical

¹ In the nest grid approach the boundary conditions of the simulations performed at finer grid size are taken from the simulation results at coarser grid size. This method is a one way approach, i.e., the information run from coarse simulation to the finer one, not vice versa. The validity of the approach become poor when reflection and resonance take place close the boundaries, i.e., when the rate of change of the bathymetry close to the boundary is high and the wave length becomes short (this can happen in case on Tsunami wave simulations). In the case of storm surge simulations, because the wave length is very high and the effect of reflections and resonance is negligible, the validity of the one way nested approach remains high also in case of near-shore simulations.

coordinate of the bottom (or bed), $\eta = z + h$ is the elevation of the free surface, g is the gravitational acceleration (opposite to the z direction)

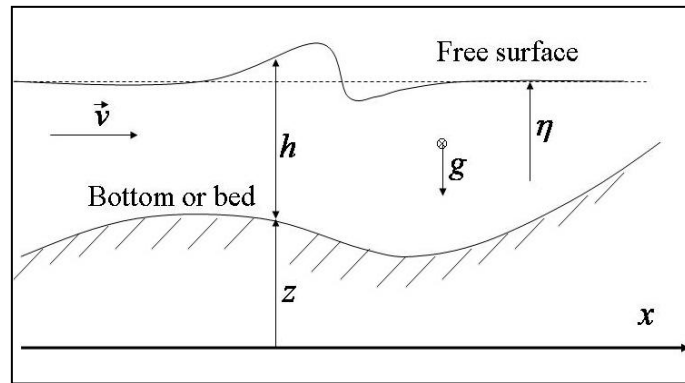


Figure 1 - Schematic of coordinate and variables of the shallow water model.

The source parameters already considered for the tsunami modeling are the bottom slope $\left\{\frac{\partial z}{\partial x}, \frac{\partial z}{\partial y}\right\}$, the Coriolis forces $\mathbf{f} = 2 \boldsymbol{\omega} \sin \theta$ (ω = rotation rate of the Earth, θ = latitude) and the bottom friction S_f expressed by the Manning formula

$$S_f = \{S_{fx}, S_{fy}\} = \frac{n^2 \sqrt{v_x^2 + v_y^2}}{h^{4/3}} \{v_x, v_y\}$$

where n is an empirical roughness coefficient for the water, called also Manning coefficient.

The source term parameters added to consider the atmospheric forcing are the parameter q for the precipitations,

S_p for the pressure and S_u for the wind friction, i.e.,

$$S_p = \{S_{px}, S_{py}\} = \frac{1}{\rho_{water} g} \left\{ \frac{\partial p}{\partial x}, \frac{\partial p}{\partial y} \right\}$$

where p is the surface pressure and S_u is given by

$$S_u = \{S_{ux}, S_{uy}\} = \frac{\rho_{air} C_D}{\rho_{water} g} \frac{\sqrt{U_{10x}^2 + U_{10y}^2}}{h} \{U_{10x}, U_{10y}\}$$

where $U_{10} = \{U_{10x}, U_{10y}\}$ are the horizontal component of the wind velocity 10m above the sea surface and C_D is the drag coefficient given by the following equation

$$C_D = \begin{cases} (0.75 + 0.067 * U_{10}) \cdot 10^{-3} & U_{10} \leq 26 \text{ m/s (Garrat, 1977)} \\ 2.18 \cdot 10^{-3} & U_{10} > 26 \text{ m/s (Powell et al., 2003)} \end{cases}$$

It is interesting to note that the parameters S_p and S_u can be seen as slopes, like the bottom friction S_f bottom slope $\left\{\frac{\partial z}{\partial x}, \frac{\partial z}{\partial y}\right\}$. In deep water the primary forcing is the atmospheric pressure deficit which causes the “inverted barometer” effect: the rise is approximately 1 cm for 1 mbar pressure drop (Pugh, 2004). Instead, as the TC approaches the coast, the surface wind stress become increasingly important and constitutes the primary forcing. Therefore the accuracy of a storm surge forecast depends on the correct estimation of the distribution of the wind and pressure fields, in particular in the vicinity of the coast.

The “radiation stress” is another forcing which is due to the presence of the short waves induced by the wind. As a result, varying (or gradient of) radiation stresses induce changes in the mean surface elevation (wave setup) and the mean flow (wave-induced currents). The radiation stresses depend on wave parameters such as wave height, wave period, and wave direction. Thus, in order to obtain accurate estimate on wave setup, it is essential to have accurate simulation of near-shore wave fields. However, several authors considered that the

radiation stress effect is negligible (see Alimov 2005): for this reason this forcing has not yet included in the hydrodynamic model.

3. ATMOSPHERIC FORCING

3.1. Data sources

Several methods have been developed to infer the pressure and wind fields, as shown in Cardone et al. (2009) and in Dube et al. (2010).

The first possibility to infer pressure and wind fields is to use the numerical weather forecasts provided at the global scale by the Global Forecast System (GFS) and the ECMWF, while GFDL and HWRF hurricane models provide forecasts at regional scale. Below a brief description of the data provided by these models is presented, while a complete description of the others TC forecasting models is in Heming et al. (2010).

The second possibility to infer pressure and wind fields is to use a parametric model. This approach develops an idealized representation of the TC, based on few key parameters. Typical parameters are the TC track (which define TC eye location and translational speed), maximum wind speed or minimum central pressure (to characterize intensity), and the radius of maximum wind (to define size). This method solves simplified equations and therefore is very robust and widely used in storm surge modeling. Several parametric models exist; the most used is the Holland's model. This model will be described in Section 3.2, while more information on the parametric models can be found in Jelesnianski et al. (1992), Thompson et al. (1996), Harper (2002) and Jakobsen et al. (2004).

In Section 3.1.1 a brief description of several forecasting data sources for the numerical weather forecast (Global Model Products and TC Model Products) and for the parametric model (TC parametric products) is presented. Instead a POST-Analysis TC parameter product (Best Track) used in our analysis is presented in Section 3.1.2. Some comparisons are given in Section 3.1.3.

3.1.1. Forecasting Products

- GLOBAL MODEL Products

The Global Forecast System (GFS): The global model of the NOAA Environmental Modeling Center of the National Centers for Environmental Prediction (NCEP) is part of the GFS. The model is based on the usual equations of conservation of mass, momentum, energy and moisture. The output is posted to a 0.5 degree equally spaced in longitude/latitude with 3-h forecast interval to 180-h, cycled 4 times per day (0000, 0600, 1200 and 1800 UTC), with 47 vertical standard pressure levels. More information are on NOAA-NCEP web site (<http://www.ncep.noaa.gov/>), Surgi et al. (1998) and Campana et al. (2005). The GFS data can be downloaded at <http://www.nco.ncep.noaa.gov/pmb/products/gfs/>.

ECMWF deterministic model: The ECMWF general circulation deterministic model, T1279 L91, consists of a dynamical component, a physical component and a coupled ocean wave component. The last operational version has a resolution approximately of 16 km. The Global forecasting products have 3-hours time interval from T+0h to T+144h, and 6-hours time interval from T+150h to T+240h. More information can be found at http://www.ecmwf.int/products/forecasts/guide/The_ECMWF_global_atmospheric_model.html.

- TC MODEL Products

GFDL TC model: The GFDL hurricane TC dynamical model is a limited-area, grid-point model designed specifically for TC prediction. The GFDL runs from an updated and improved version of NCEP global model, it obtains its boundary conditions from a global dynamical model such as GFS and it is coupled with the Princeton Ocean Model (POM). The current GFDL hurricane model consists of a triply-nested grid configuration: the outermost grid spans 75°x75° with 1/2° of resolution; the middle grid spans 11°x11° with 1/6° of resolution; while the innermost grid spans 5°x 5° with 1/12° of resolution. The GFDL hurricane forecasts are produced every six hours (00, 06, 12, and 18 UTC) out to 126 hours for up to four TCs at a time. These forecasts are available about five hours after the primary and intermediate synoptic times (0000, 0600, 1200 and 1800 UTC). More information can be found at GFDL web site (<http://www.gfdl.noaa.gov/>) and the model data can be downloaded from the NCEP ftp server (<ftp://ftp.ncep.noaa.gov/pub/data/nccf/com/hur/prod/>).

HWRF TC model: Development of this model began in 2002 at the NCEP - Environmental Modeling Center (EMC) in collaboration with the GFDL scientists and the University of Rhode Island. HWRF is a non-hydrostatic coupled ocean-atmosphere model, which utilizes highly advanced physics of the atmosphere, ocean and wave. It makes use of a wide variety of observations from satellites, data buoys, and hurricane hunter

aircraft. The ocean initialization system uses observed altimeter observations, while boundary layer and deep convection are obtained from NCEP GFS. The current HWRF model has a nested grid system with an outermost domain and a nested grid with resolutions of 27 and 9 km respectively, 42 vertical levels and a domain of 75° x 75°. The HWRF provides operational guidance for forecasters at the NHC in both the Atlantic and East Pacific basins. The hurricane forecasts are produced every six hours (00, 06, 12, and 18 UTC). These forecasts are available about five hours after the primary and intermediate synoptic times. More information can be found at: <http://www.emc.ncep.noaa.gov/HWRF/index.html> and the data can be downloaded at <http://www.nco.ncep.noaa.gov/pmb/products/hur/>

- ***TC PARAMETER Products***

The most important sources of TC information are the TC bulletins provided by the Regional Specialized Meteorological Centres (RSMCs) and the Tropical Cyclone Warning Centres (TCWCs) (Appendix A). These centers have the regional responsibility to forecast and monitor each area of TC formation. Every 6-hours the TC warning centers publish a TC bulletin, including information such as wind speed, pressure, and track locations which are used as input for the parametric models (e.g. Holland's model). The information and format, included in each bulletin, vary from center to center (Knaff et al., 2010; RSMC and TCWS web sites). The Pacific Disaster Centre (PDC) set up an automatic routine which includes TC bulletins from all RSMCs into a single database covering all TC basins (JRC GDACS database).

NOAA NHC bulletin and GDCAS database are described below. In addition to the RSMC and TCWC also other organizations such as the Joint Typhoon Warning Center (JTWC) and the ECMWF, provide to the public information about TCs to the public. These products are described below.

NOAA NHC bulletin: NHC issues tropical and subtropical cyclones every six hours at 0300, 0900, 1500, and 2100 UTC. The covered areas are the Atlantic and eastern Pacific Oceans. The NHC bulletin contains a list of all current watches and warnings on a tropical or subtropical cyclone, as well as the current latitude and longitude coordinates, intensity, and system motion. The intensity includes the analysis of the central pressure (it is not forecasted), and the maximum sustained (1-min average) surface wind analyzed and forecasted for 12,24,36,48, and 72 hours. The wind radii for 34 and 50 knots are forecasted through 72 hours, while the 64-knot radii are forecasted through 36 hours. More information are on the NOAA-NHC web site (<http://www.nhc.noaa.gov/>), while a validation of the NHC products are in Cangialosi et al. (2011) and Rappaport et al. (2009).

JTWC bulletin: The [Joint Typhoon Warning Center \(JTWC\)](http://www.usno.navy.mil/JTWC/) is the U.S. Department of Defense agency responsible for issuing tropical cyclone warnings for the Pacific and Indian Oceans. TC bulletins are issued for the Northwest Pacific Ocean, North Indian Ocean, Southwest Pacific Ocean, Southern Indian Ocean, Central North Pacific Ocean. JTWC products are available by 03Z, 09Z, 15Z, or 21Z (in the North Pacific and North Indian Ocean tropical cyclone warnings are routinely updated every six hours, while in South Indian and South Pacific Ocean are routinely updated every twelve hours). The bulletins include position of TC center, the maximum sustained wind based on 1-min average and the wind radii. More information can be found at (www.usno.navy.mil/JTWC/).

JRC GDACS database: The data in the TC's bulletins are not available in a single standard format, so they are difficult to use in an automatic system like GDACS. To overcome this problem, PDC set up an automatic routine which includes TC bulletins from all RSMCs into a single database covering all TC basins (Vernaccini et al., 2007; <http://www.pdc.org>). The NOAA bulletins are included for Atlantic, Eastern Pacific and Central Pacific basins, while the JTWC bulletins are included for the rest of the world.

ECMWF Tropical Cyclone forecast product: it is designed to provide both deterministic and probabilistic information on movement and intensity of individual TC. The system depends on observations from various TC centres around the world. Once observations are available, the movement of a TC is automatically tracked, both in the deterministic and the EPS forecasts. The tracking algorithm is based on extrapolation of past movement and the mid-tropospheric steering flow to obtain a first guess position. ECMWF's TROPICAL CYCLONE trajectory forecast products have 6-hours time interval and provide the latitude and longitude of the TC center, P_c , V_{max} with its position. More information can be found in Van Der Grijin (2002) and at http://www.ecmwf.int/services/dissemination/3.1/TROPICAL_CYCLONE_trajectory_forecast_products.html.

3.1.2. Post-Analysis Products

Below only one post-analysis product, which provides TC parameters that can be used as input in Holland's model, is shown. More information on post-analysis products can be found in Cardone et al. (2009) and in Heming et al. (2010).

- *TC PARAMETERS Product*

The first sources of post-analysis data are the **Best Track (BT)** databases, where all the information required by the Holland's model to infer the wind and pressure fields are included. BT data are provided by the TC's Warning Centers. These datasets contain the best information available on several TC's information such as TC's center position, intensity and other parameters (e.g. wind radii), obtained from observational and model data. An example of BT database is the NOAA's hurricane database (or HURDAT). It is the official record of TCs for the Atlantic Ocean, Gulf of Mexico and Caribbean Sea (HURDAT website, www.aoml.noaa.gov/hrd/). NOAA best track data can be also downloaded from the Automated Tropical Cyclone Forecast (ATCF) database at <ftp://ftp.nhc.noaa.gov/atcf/archive/>. This dataset contains the best available six-hourly representative estimates of several parameters such as track, V_{max} , P_c , R_{max} and wind radii. Recently a new project of NOAA, International Best Track Archive for Climate Stewardship (IBTrACS), was formed under the auspices of the World Data Center for Meteorology–Asheville. This project combines TC's BT data from all agencies into an integrated dataset readily available to the user community. The intent of the IBTrACS project is to overcome data availability issues and to freely disseminate a new global dataset. More information are in Knapp et al. (2010) and on IBTrACS website (<http://www.ncdc.noaa.gov/oa/ibtracs/index.php>).

3.1.3. Atmospheric data set comparisons and discussion

In this Section the NOAA GFS and GFDL products are compared to show how these products simulate the pressure and wind fields. They are also compared with the output of the Holland's model, using as input Best Track data, to show how this parametric model simulates these fields. A complete evaluation of GFS, GFDL and Holland's model can be found in Harper et al. (2001), Bender et al. (2007) and Heming et al. (2010). The data sources used are: NOAA GFS (0.5°), GFDL hurricane ($1/12^\circ$) and NOAA Best Track.

The parameters compared are: mean sea level pressure (*mslp*) and surface wind speed ($u10$, $u10x$ and $u10y$), where the wind-level of the GFS and NOAA Best Track data is 10-m, while that of GFDL is 35-m. The TC analyzed is Earl, occurred in 2010 in the North Atlantic basin (Cangialosi, 2011).

Some comparisons on Earl forecasted data (1st September 2010 12:00 UTC) are presented in Figure 2 - Figure 4.

Figure 2 shows the *mslp* (a) and $u10$ (b) field of GFS (top panel), GFDL (middle panel) and Holland's model (bottom panel). Figure 2.a shows that the GFS resolution (0.5°) is too coarse to simulate the pressure gradient inside a TC. The GFS simulate a P_c of only 986 mbar, while the Best Track value is 943 mbar. The difference is of 43 mbar. On contrary the P_c simulated by GFDL is very similar to Best Track data. The difference is only 5 mbar. The *mslp* field derived from the NOAA Best Track data using the Holland's model (Section 3.2) is very similar to GFDL *mslp* field. Also the GFDL $u10$ field is very similar to the Holland's model $u10$ field. Both fields are asymmetric, due to the effect of translational velocity, and both models simulate a V_{max} more than 55 m/s. Also the $u10$ field of GFS is asymmetric, but it doesn't reproduce correctly the value of V_{max} . The value of V_{max} for the GFS is lower than 40 m/s. Therefore, as for the *mslp* field, the GFS resolution (0.5°) is too coarse to reproduce accurately the $u10$ field. Instead the GFDL model with a resolution of $1/12^\circ$ is able to represent accurate *mslp* and $u10$ fields.

The GFS resolution is also too coarse to represent the two components of $u10$, $u10x$ (Figure 3.a) and $u10y$ (Figure 3.b).

Figure 4 shows the *mslp* (a), $u10$ (b), $u10x$ (c) and $u10y$ (d) profiles for the latitude of TC center. The minimum of pressure in Figure 4.a represents the pressure of TC center (P_c). As in Figure 2.a, the GFS is not able to reproduce this parameter, while the results of GFDL and Holland's model are very similar. As in Figure 2.b, the GFS is not able to reproduce adequately V_{max} . The figures of the two components of $u10$, $u10x$ (Figure 2c) and $u10y$ (Figure 2d), show that an effect determines an "inflow angle". More information on this effect can be found in Section 3.2.

In Table 1 the values of TC's center location (latitude and longitude), V_{max} and P_c are presented for the three data sets analyzed (GFS, GFDL, and Best Track). The position of the TC's center of GFS and GFDL model corresponds at the position of the minimum of the pressure field obtained analyzing the pressure field.

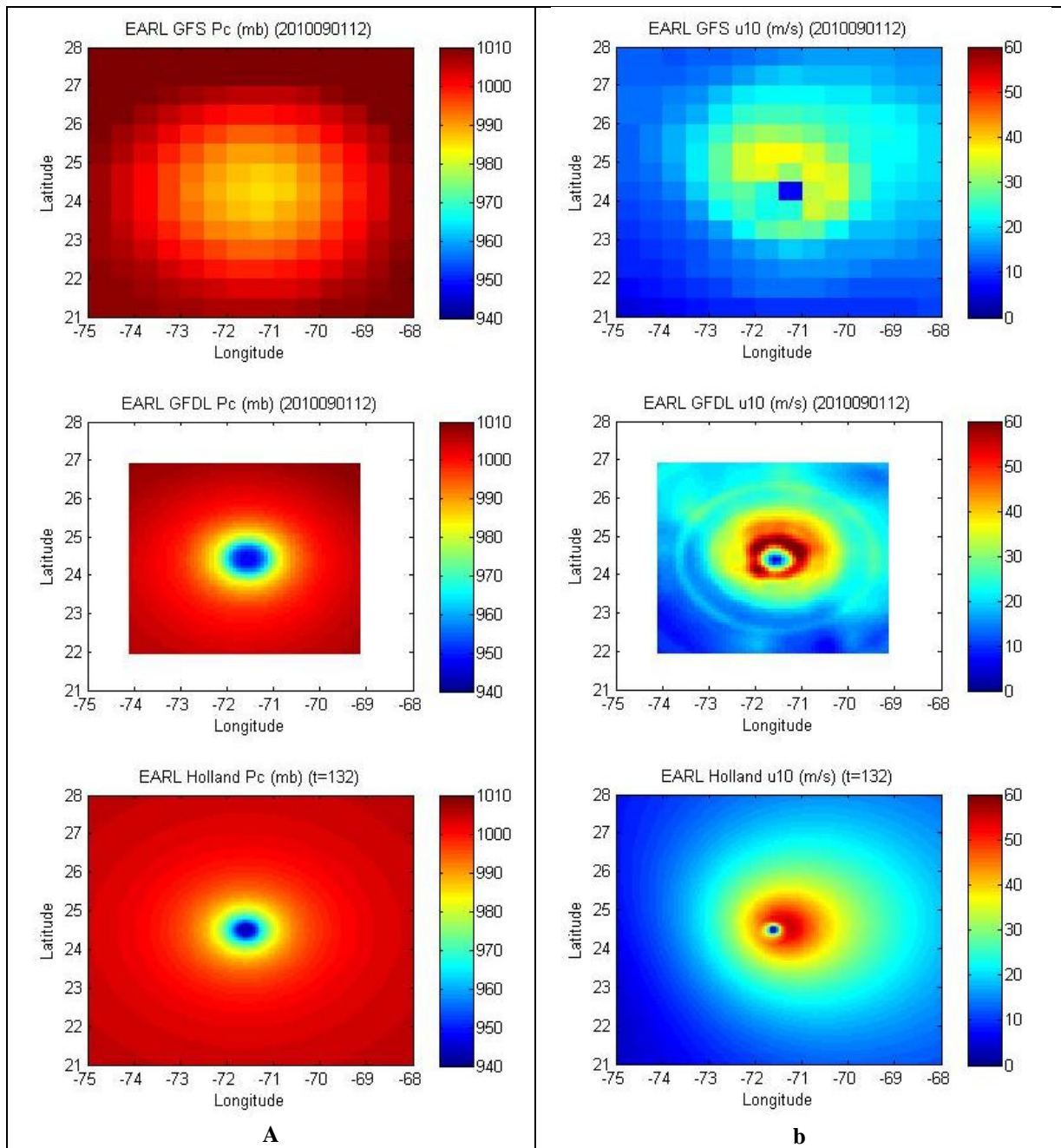


Figure 2 - EARL's surface pressure field (a) and 10m level wind field (b) from GFS (top), GFDL (middle) and Holland (Bottom) data for the 1st of September 2010 (12:00 UTC).

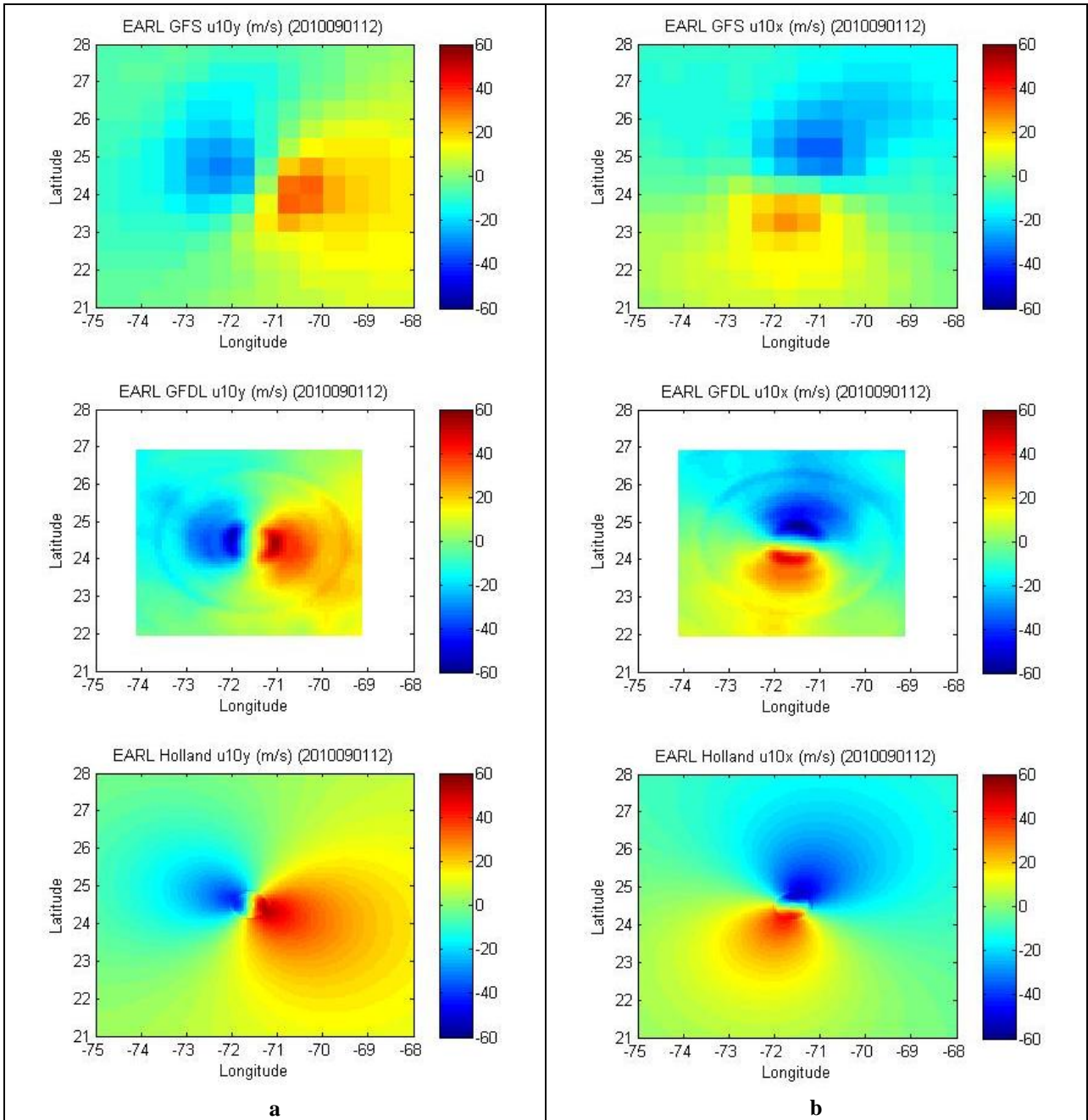


Figure 3 - Same as Figure 2 but for x-component (a) and y-component of the 10m level wind field.

09/01/2010 (12:00 UTC)	Longitude	Latitude	P _c (mbar)	V _{max} (m/s)
BEST TRACK	-71.60	24.50	943	56.6
GFS (0.5°)	-71.25	24.25	986	37.5
GFDL (1/12°)	-71.58	24.48	948	66.9

Table 1 – Track (Longitude and Latitude), P_c and V_{max} of TC Earl using different data sets for the 1st of September 2010 (12:00 UTC).

The comparisons presented in Figure 2 to Figure 4 show that the GFS model does not simulate accurately the pressure and wind fields: the reason is that the global atmospheric models were not designed to resolve the extreme pressure gradients associated with TCs (Van Der Grijin, 2002), (Kuroda, et al., 2010). However, the global models are widely used for TC's track predictions (Dube, et al., 2010). Recently, several improvements have been made to the global models resolution. The new version of the NOAA global model has a resolution of 27 km, while that of ECMWF is 16 km. After this recent improvement, the global models could be able to reproduce the extreme gradient inside a TC as shown in (Miller, 2010). In future these global products could be used to reproduce the accurate atmospheric forcing in storm surge modeling.

TC models, GFDL and HWRF, use a high resolution nested grid, around 10 km, to represent the storm's dynamics, therefore they can predict adequately TC's track and intensity. These models reproduce adequately the pressure and wind fields that could be inputted to storm surge codes like HyFlux2: unfortunately these data sets are not available in each TC's basin.

Concluding the atmospheric forecast products, like GFDL regional products, which provide an accurate pressure and wind fields, are not yet globally available, or are available only for post-analysis. Therefore the Holland's model seems at the moment the more advantageous choice to infer the pressure and wind fields for the global storm surge forecasts requested by GDACS.

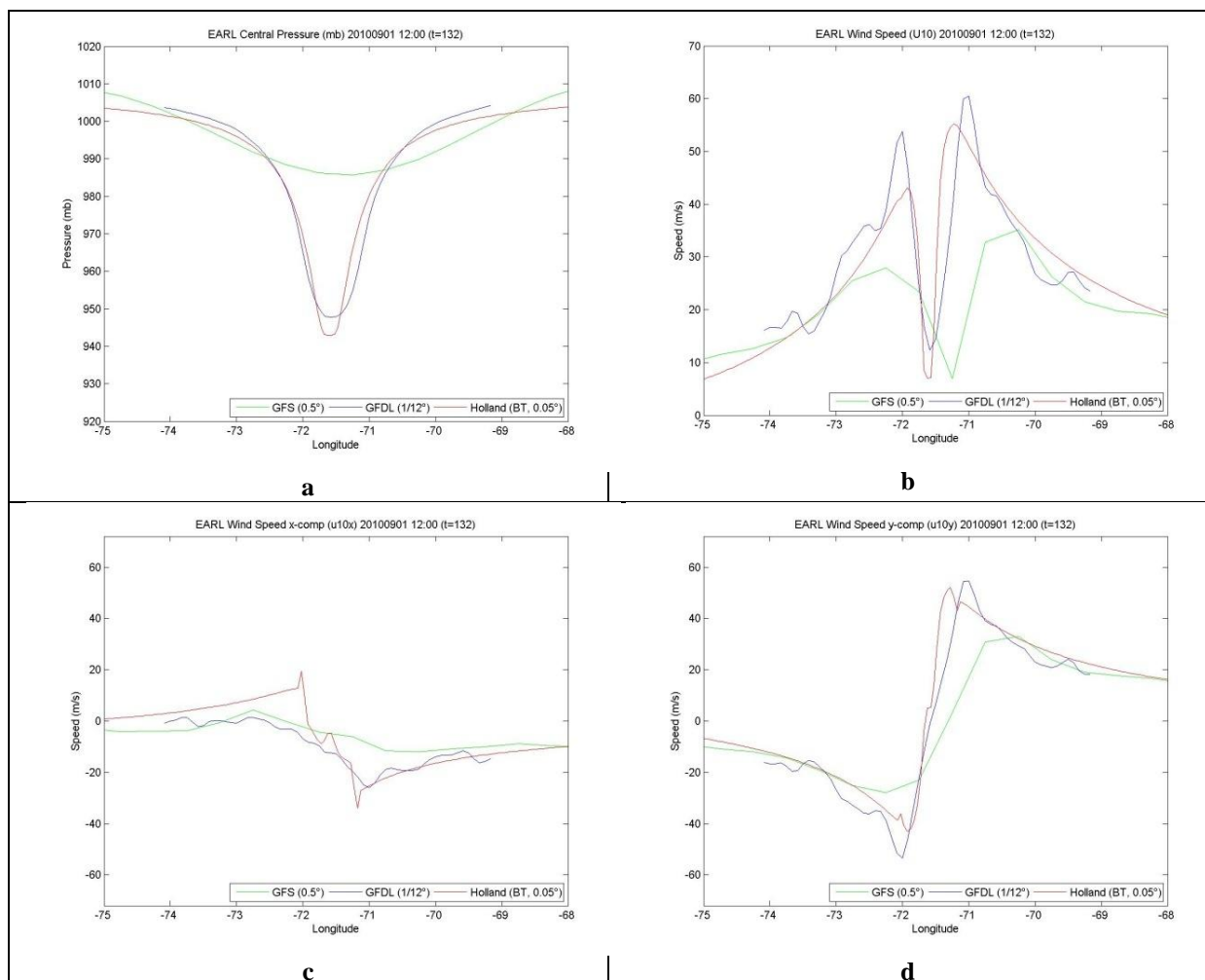


Figure 4 - EARL's pressure (a), wind speed (b), x-(c) y-(d) component of wind speed for the latitude of the TC center for the 1st of September 2010 (12:00 UTC).

3.2. Holland's parametric model

The Holland's model (Holland, 1980) is the most widely used parametric model in storm surge modeling (Tang et al., 1997; Vickery et al., 2009). Below a brief description of the model with the recently improvements of Holland (Holland et al., 2010) are presented.

MODEL CHARACTERISTICS (HOLLAND 1980)

The primary assumption of Holland's model (Holland, 1980) is that for a generic TC the surface pressure field follows a modified rectangular hyperbola as a function of radius (Schloemer, 1954). The pressure field is then obtained from the following equation:

$$P(r) = P_c + (\Delta P) e^{-\left(\frac{R_{max}}{r}\right)^B} \quad (2)$$

where:

- $P(r)$ = surface pressure at a distance r from the TC's center (Pa);
- $\Delta P = P_n - P_c$ = Pressure drop (Pa);
- P_c = central pressure (Pa);
- P_n = environmental pressure (usually taken as the pressure of the last closed isobar, Pa);
- R_{max} = radius of maximum wind (m);
- B = Scaling factor (peakedness), it defines the pressure and wind profile shape (1÷ 2.5).

The gradient level winds are then derived by considering the balance between the centrifugal and Coriolis forces acting outward and the pressure force acting inward.

$$\frac{V_g^2(r)}{r} + f V_g(r) = \frac{1}{\rho_{air}} \frac{dP(r)}{dr} \quad (3)$$

where:

- $V_g(r)$ = gradient level wind at a distance r from the TC's center (m/s);
- f = Coriolis parameter: $f = 2 \omega \sin \varphi$;
- ω = rotation rate of the Earth (7.2722054×10^{-5} rad/s) ;
- φ = latitude;
- ρ_a = air density.

In Holland (1980) the air density is assumed constant (1.15 kg/m^3)².

By substitution of the pressure gradient obtained from Equation (2) into the balance of forces Equation (3) and solving in respect the gradient wind field (V_g), the following is obtained:

$$V_g(r) = \left[\frac{B}{\rho_a} \left(\frac{R_{max}}{r}\right)^B (\Delta P) e^{-\left(\frac{R_{max}}{r}\right)^B} + \left(\frac{rf}{2}\right)^2 \right]^{1/2} - \frac{rf}{2} \quad (4)$$

In the region of maximum winds where the Coriolis forces are small in comparison to the pressure gradient³ the previous equation becomes:

$$V_c(r) = \left[\frac{B}{\rho_a} \left(\frac{R_{max}}{r}\right)^B (P_n - P_c) e^{-\left(\frac{R_{max}}{r}\right)^B} \right]^{1/2} \quad (5)$$

² This is not a strong assumption if one considers that, in an adiabatic expansion, for a change of pressure of 100 mbar the change of density is 0.08 kg/m³, i.e., less than 8 %.

³ the air is in Cyclostrophic balance, i.e., the pressure gradient is compensated by the centrifugal force (Holton, 2004)

The maximum wind speed (V_{max}) is the wind speed at a distance equal to R_{max} , therefore by substitution of r with R_{max} in Equation (4) one obtain

$$V_{max} \approx \sqrt{\frac{B \Delta P}{e \rho}} \quad (6)$$

From this equation the Holland's parameter B can be derived as following:

$$B = \frac{V_{max}^2 \rho_a e}{P_n - P_c} \quad (7)$$

The Holland (1980) model is axis-symmetric, so several additional phenomena must be taken into account in order to model the real asymmetry of the wind field. Factors that can contribute to the asymmetric structure of a TC are the friction and the TC's system motion. Since 1980, several improvements have been made to take in to account these factors. Following the most important improvements are presented, while a complete state-of-the art are in Harper et al. (2001).

Theoretically, surface friction in marine waters must be included when converting the gradient winds⁴ to surface winds. In order to obtain the surface winds, a boundary layer wind speed and an inflow direction correction has to be applied to the gradient winds.

The adjustment to the surface (boundary layer correction) is based on the logarithmic deficit law approach, whereby the near-surface boundary layer profile at any height z is a function of the surface roughness z_0 and the reference wind speed (Powell, 1980). These assumptions permits to calculate surface (at +10 m) velocity (V_s) using a boundary layer coefficient (Harper et al., 2001). Recently (Holland et al., 2010) proposed a (revised) model to describe directly the surface wind profile, incorporating into the equation the boundary layer effects.

The inflow angle correction ($+\beta$ in Southern Hemisphere, $-\beta$ in Northern Hemisphere) is applied to represent the cross-isobaric flow caused by surface friction (Harper et al., 2001). Usually this correction is approximately 25° in the outer region, but reduces to zero near the radius of maximum wind. In the method presented in this work, the following values proposed by Harper et al. (2001) are used:

$$\beta = \begin{cases} 10 * \left(\frac{r}{R_{max}}\right) & 0 \leq r < R_{max} \\ 10 + 75 * \left(\frac{r}{R_{max}} - 1\right) & R_{max} \leq r < 1.2 R_{max} \\ 25 & r \geq 1.2 R_{max} \end{cases} \quad (8)$$

More information can be found in Shea et al. (1973) and Sobey et al. (1977).

The movement of the TC is one of the factors which produce complex changes to the surface winds. Therefore the moving velocity vector of the TC (translational velocity, V_t) is added to the surface wind speed, reproducing the cyclone's asymmetry. In order to take into account that the translational effect of the TC disappears in the region far from the cyclone eye, the speed V_t is multiplied by a weight that decays exponentially with the distance r .

When a TC is inland, another factor must be included to simulate the wind field. Kaplan et al. (1995) developed an empirical model to predict the maximum wind of TC's land falling. More information are in Powell et al. (1996) and Bhowmik et al. (2005). Inland phenomena are not included in the model used at JRC to infer the atmospheric forcing because for storm surge simulation only the interactions between wind and marine water are taken into account.

MODEL REVISED (HOLLAND 2010)

Recently Holland et al. (2010) proposed a revised model able to reproduce surface wind fields with height accuracy, eliminating the needs of first calculating the gradient wind and then reducing this field to the surface by taking into account the boundary layer effects. They introduce a variable exponent x to simulate the wind in the core (where the effect of the boundary layer is considered negligible) and the external regions. Therefore, the wind field is given by:

$$V_s(r) = \left[\frac{B_s}{\rho_{as}} \left(\frac{R_{max_s}}{r}\right)^{B_s} \Delta p_s e^{-\left(\frac{R_{max_s}}{r}\right)^{B_s}} \right]^x \quad (9)$$

⁴ Non-geostrophic winds which blow parallel to isobars, **where there are no frictional forces**, and the pressure gradient and Coriolis forces are compensated by the centrifugal forces

where the subscript s refers to the surface values at a nominal height of 10 m.

In the previous Holland's model the value of x was fixed at 0.5 and it was impossible to simulate correctly the wind in both regions (Willoughby, et al., 2004). In Holland et al. (2010) they show how the profile could be adjusted using the following expression

$$x = \begin{cases} 0.5 & r \leq R_{max} \\ 0.5 + (r - R_{max}) \frac{x_n - 0.5}{r_n - R_{max}} & r > R_{max} \end{cases} \quad (10)$$

where x_n is the adjusted exponent used to fit the peripheral observations at radius r_n .

This new revised version simulates the whole wind profile (core and external) and includes also a capacity to incorporate additional wind observations at some radius.

CONSIDERATIONS

In Table 2 the required Holland's parameters are shown. When the model is used to simulate the pressure and wind fields of an historical TC the post-analysis best tracks data can be used to derive the requested parameters. Instead when Holland's model is used as a "forecasting model", there are some critical points, because some of the Holland's parameters (e.g. ΔP , R_{max} , B) are not always available in the TC bulletins.

Several methods have been developed to estimate B (e.g. Vickery et al., 2000; Harper et al., 2001; Jakobsen et al., 2004; Vickery et al., 2008), because it plays an important role in TC's modeling, modulating both the maximum wind speed and the shape of the outer wind profile.

Operational TC's centers throughout the world use different wind-pressure relationships (Harper, 2002; Courtney et al., 2009) to determine V_{max} and P_c . A complete description of these relationships is presented in Knaff et al. (2010), while in Knaff et al. (2007) the most used are reexamined. Various factors influence these pressure-wind relationships (Kieu et al., 2010). Moreover there is a lack of suitable observational data that makes validation difficult (Knaff et al., 2007; Knaff, et al., 2010). These empirical relationships are not used in the JRC method.

Parameter	Symbol	Units
Time	<i>time</i>	s
Latitude	θ	°
Longitude	λ	°
Central pressure	P_c	Pa
Environmental pressure	P_n	Pa
Radius of maximum wind	R_{max}	m
Maximum wind velocity	v_{max}	m/s
B (peakedness's factor)	B	-
X (scaling factor to adjust the profile shape)	x	-

Table 2 - Holland's model parameters.

In addition to the TC bulletins there is also the ECMWF TC trajectory forecast product which provides P_c , V_{max} and the location of the TC center as well as the location of the area of maximum winds. Several studies show that the ECMWF model simulates very well the TC track (Tyagi, et al., 2010), but the coordinates of the area of maximum wind (used to infer R_{max}) are not provided with height accuracy. Moreover this product is not free-downloadable.

In Table 3 the Holland's parameters availability for Best Track, Bulletins and ECMWF datasets are presented. As shown in this Table there is a lack of a global and free downloadable dataset which provides the Holland's parameters. This has led the JRC to develop a method to determine the Holland's parameters using the wind Radii data, which are available since the past decade in each TC bulletins.

	TC	Best Track	Bulletins		ECMWF TC trajectory
			Advisory ($t=0$)	Forecast	
V_{max}	KATRINA	x	x	x	-
	NARGIS	x	x	x	x
	YASI	x	x	x	x
	EARL	x	x	x	x
R_{max}	KATRINA	x	-	-	-
	NARGIS	x	-	-	x
	YASI	-	-	-	x
	EARL	x	-	-	x
ΔP	KATRINA	x	x	-	x
	NARGIS	x	-	-	x
	YASI	-	-	-	x
	EARL	x	x	-	x

Table 3 - Holland's parameters availability in Best Track, TC bulletins and ECMWF dataset.

3.3. Wind radii treatment

JRC has developed a Monte Carlo method to infer the Holland's parameters not available in the TC bulletins (e.g. R_{max} , ΔP , B , x) using the wind radii data archived in JRC database. Following a description of this method with some validation is presented. The derived Holland's parameters are used to infer the pressure and wind fields in the HyFlux2 storm surge simulations.

DESCRIPTION

This method is based on the recently revised Holland's model (Holland et al., 2010) described in Section 3.2 using as input the information provided in each TC bulletins: the coordinates of TC center (Lat and $Long$), maximum of wind speed at 10m level (V_{max}) and the three wind radii at each quadrant (velocity indicates as V , radius as R_{34} , R_{50} , R_{64}). This TC information's is inferred from the JRC database. In this database the velocities are 1-min averaged, therefore they are multiplied by a factor of 0.8-0.9 (Holland, 2008) to convert them in 10-min average. More information can be found in Harper (2002) and Harper et al. (2010).

Following is the Holland's equation (Eq. 11) which provides the surface wind profile not including the Coriolis effect and the translational velocity.

$$V(R) = \left[\frac{B}{\rho_a} \left(\frac{R_{max}}{r} \right)^B \Delta p e^{-\left(\frac{R_{max}}{r} \right)^B} \right]^x \quad (11)$$

$$x = 0.5 + \frac{r - R_{max}}{Max(r) - R_{max}} * k \quad (12)$$

where:

- V = wind radii velocity expressed in m/s
- r = radius of wind radii (km)
- R_{max} = Radius of maximum wind (km)
- Δp = Pressure drop expressed in Pa (1 Pa = 10^{-5} bar)
- ρ_a = air density = 1.15 kg/m³
- B = Peakedness's factor
- x = scaling factor to adjust the profile shape
- k = coefficient between 0 and 0.15
- $Max(r)$ = 500 km

An important consideration has to be pointed out if the Holland's Equation is used to simulate all the quadrants (NE , NW , SW , SE) at the same time: the wind radii data and V_{max} include the translational velocity of TC; therefore this effect has to be subtracted from the wind radii data when the Eq. 11 is used.

The translational velocity (V_t) and the angle of motion (φ) are calculated from the TC positions (latitude and longitude) at time t . The translational velocity is multiplied⁵ by a weight (w_f) that decays exponentially with the distance from the TC eye (r) as follow:

$$Vt_{wf} = V_t * w_f \quad (13)$$

$$w_f = 1 - e^{-\left(\frac{R_{max0}}{r}\right)^{B_0}} \quad (14)$$

where:

- Vt_{wf} = translational speed of the TC center multiplied by an exponential weight;
- V_t = translational speed of the TC center;
- w_f = weight that decays exponentially with the distance from the TC eye center;
- r = distance from the TC eye center;
- $R_{max0} = 20km$;
- $B_0 = 1.5$.

The translational velocity ($\bar{V}t_{wf}$), obtained from Equation 13, is then projected on the direction of the tangential wind velocity ($\bar{\tau}_Q$) in each quadrant (Q). Therefore the translational velocity in each quadrant ($Vt_{\tau Q}$) is calculated as follow:

$$Vt_{\tau Q} = \bar{V}t_{wfQ} \cdot \bar{\tau}_Q = Vt_{wfQ} * [\cos(\varphi) * \cos(\theta'_Q) + \sin(\varphi) * \sin(\theta'_Q)] \quad (15)$$

where:

- Q = Quadrant = *NE, NW, SW, SE*
- θ_Q = Quadrant Angle: $\theta_{NE} = 45^\circ$, $\theta_{NW} = 135^\circ$, $\theta_{SW} = 225^\circ$, $\theta_{SE} = 315^\circ$;
- θ'_Q = Angle of tangential wind velocity = $\theta_Q + 90^\circ$;
- φ = Angle of TC center motion calculated counterclockwise respect the correspondent line of parallel.

Finally the translational velocity obtained is subtracted from the wind radii velocity. The Coriolis effect is also subtracted from the wind radii, since this effect is not included in the Eq. 11. The same is done for the maximum velocity. The obtained wind radii and V_{max} are then used in a Monte Carlo method to infer the value of R_{max} , ΔP , B , x . Firstly N random triplets R_{max} , ΔP and k are created by a random no. generator, with the minimum and maximum value shown in Table 4. Then for each couple of R_{max} and ΔP the Holland's parameter B is calculated using the Eq. 7.

The N values of R_{max} , ΔP , x and B are introduced in Eq. 11 to obtain the wind speeds at distances R_{34} , R_{50} , R_{64} . The parameters that minimize the root-mean-square error (RMSE) are chosen as input for the Holland's model to simulate wind and pressure fields.

For $N < 10^4$ the results can vary significantly (Figure 5). In this figure the results of R_{max} and ΔP for TC Earl, obtained varying N , are presented. For a value of $N \geq 10^4$ the results became similar. Same considerations are found comparing the BIAS and RMSE, as shown in Figure 6. For $N < 10^4$ the RMSE varies significantly (Figure 6b). However, for any value of N , the RMSE is of the same order of the step for which V_{max} is provided in the TC bulletins, which is around 5 knots. The time required to apply the method for each set of wind radii, using $N = 10^4$, is few seconds.

Parameter	Minimum value	Maximum value
$R_{max} (m)$	5000	Min (R) * 0.99
$\Delta P (mbar)$	5	200
$k (-)$	0	0.15
$B (-)$	0.8	1.8

Table 4 -Minimum and maximum value used in the Monte Carlo method.

⁵ This is done in order to take into account that the effect of the movement of the tropical cyclone should become negligible for high distance from the eye. For this purpose the decay law is similar to the pressure decay law.

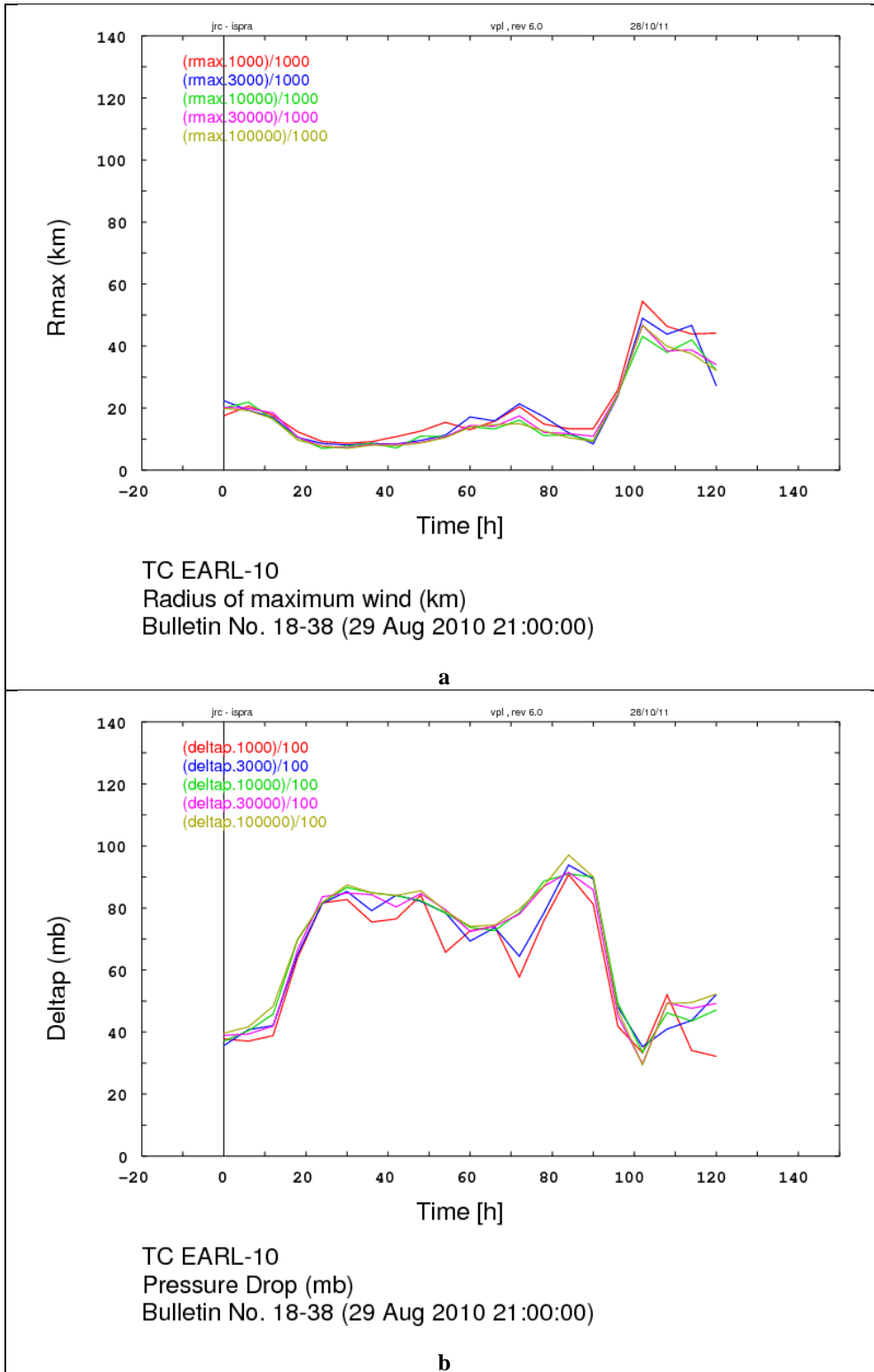


Figure 5 - Radius of Maximum wind and Pressure Drop of Earl of Bulletins 18-38, obtained from the wind radii treatment varying N.

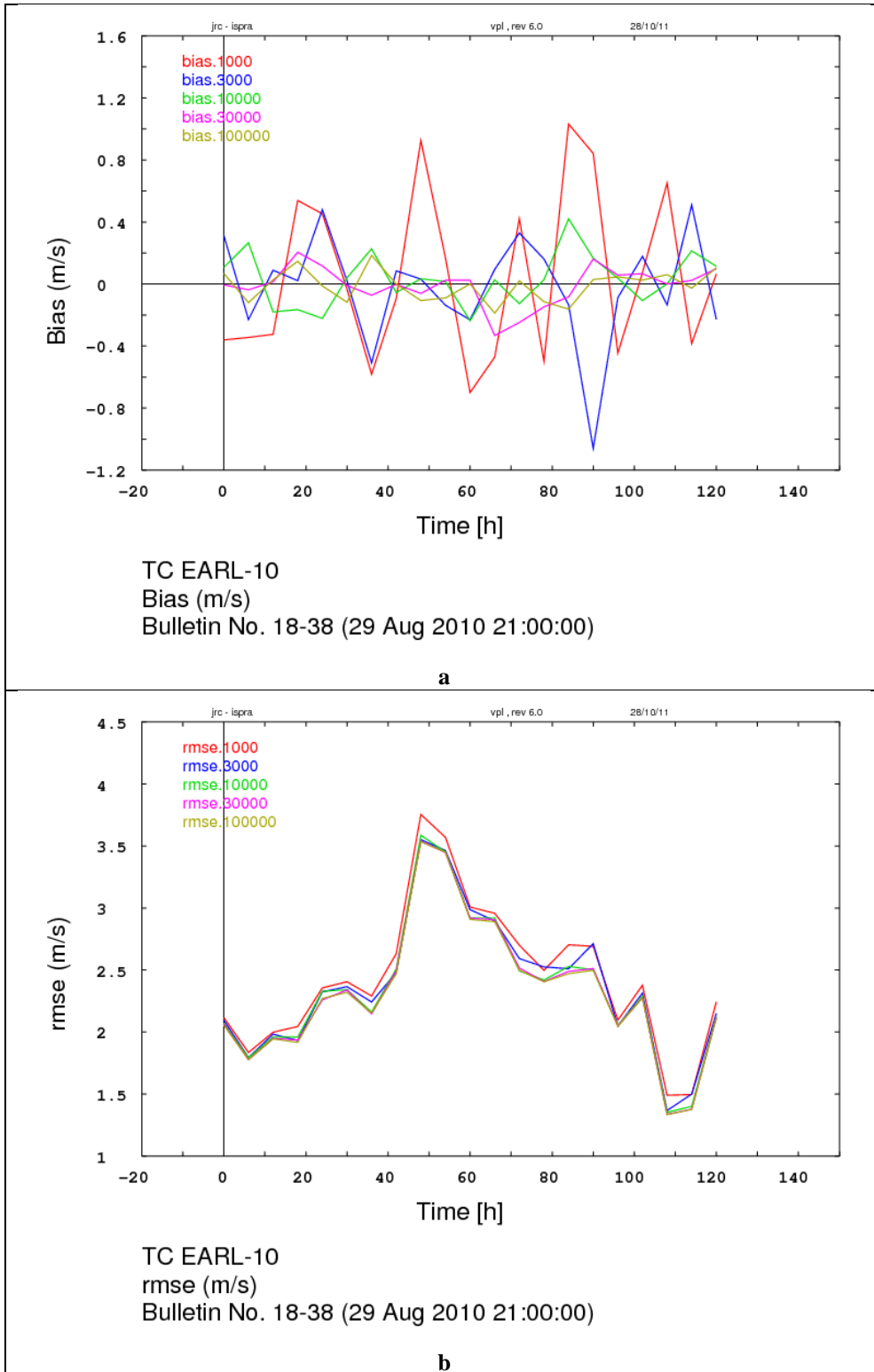


Figure 6- BIAS and RMSE of EARL of Bulletins 18- 38 obtained from the wind radii treatment varying N.

RESULTS AND DISCUSSION

Some results obtained from the wind radii treatment for the TCs Earl, Nargis and Katrina are presented below. The advisories (time 0) of the TC bulletins provided in GDACS database are used as input for the wind radii treatment for Earl and Nargis, while NOAA Best Track are directly used for Katrina.

Two examples of wind profile obtained from the wind radii treatment are presented, then the parameters obtained from the wind radii treatment, using all the advisory data (time 0) of each TC bulletin for TC Earl and Nargis, are compared with the Best Track data. NOAA Best Track data are used for Earl and Katrina while RSMC (New Delhi) and JTWC best track data are used for Nargis (only the Pressure Drop obtained for both TCs are presented in this Section).

In Figure 7 the Earl’s wind profile on 1st September 2010 (15:00 UTC) is presented, in Figure 8 the Nargis wind profile on 30 April 2008 (12:00 UTC), while in Figure 9 the Katrina wind profile on 27 August 2005 (12:00 UTC). In these figures the blue line represents the wind profile calculated using the Holland’s parameters obtained from the wind radii treatment, while the red marks represent the wind radii data. The Coriolis effect and the translational velocity are subtracted from the wind profile and from the wind radii data.

RMSE and BIAS obtained from the wind radii are very low, for both TCs, as shown in Table 5. The BIAS is negligible while the RMSE is in the order of 1-3 m/s, which is lower than 10 % of the wind velocity.

Tropical Cyclone	Advisory time	RMSE	BIAS
EARL	1 September 2010 (15 UTC)	2.69	0.092
NARGIS	30 April 2008 (12 UTC)	0.78	-0.060
KATRINA	27 August 2005 (12 UTC)	1.35	-0.051

Table 5 - Examples of RMSE and BIAS for EARL, NARGIS and KATRINA.

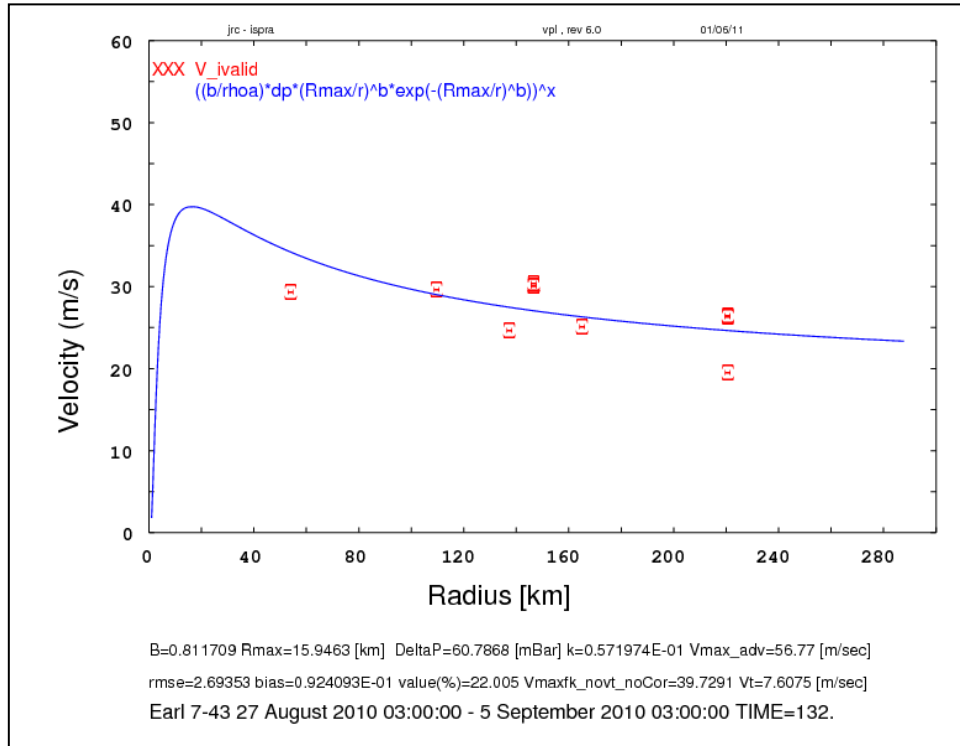


Figure 7 –EARL’s wind profile obtained from the wind radii treatment (1 September 2010 15:00 UTC).

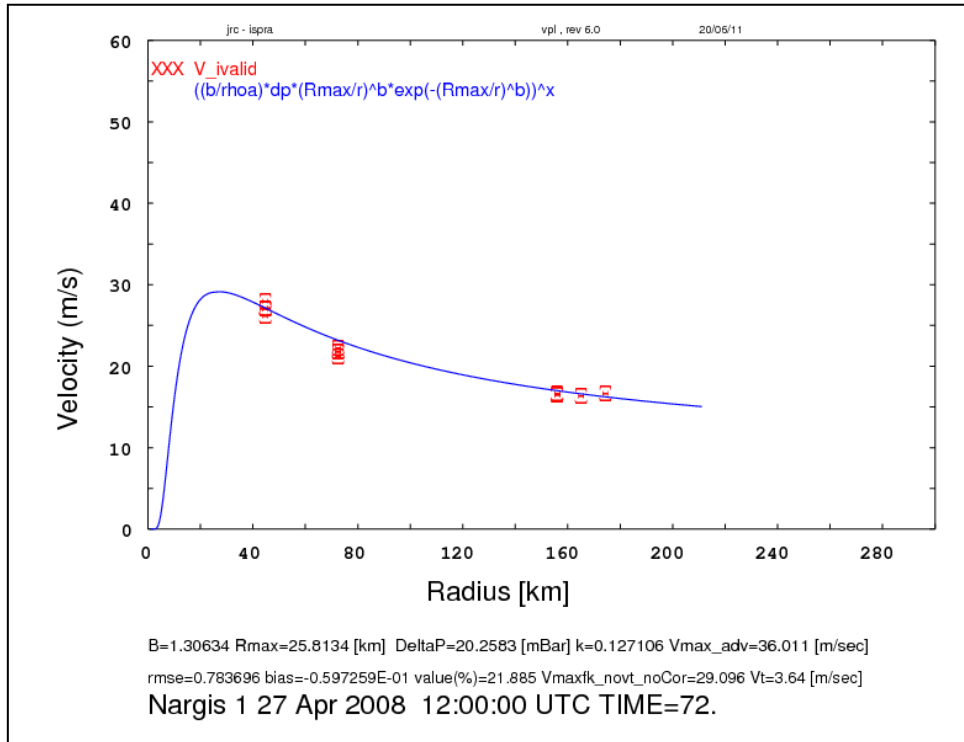


Figure 8 – Same as Figure 7 for TC Nargis (30 April 2008 12:00 UTC = 27 April 2008 12:00 UTC +72 h).

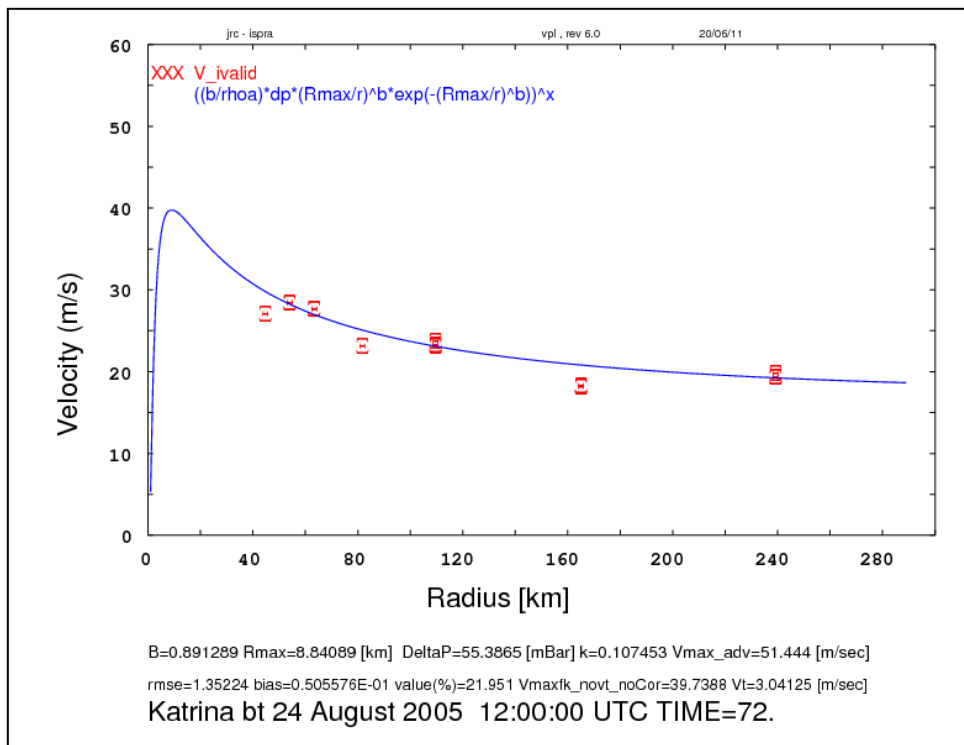


Figure 9- Same as Figure 7 for TC Katrina 27 August 2005 12:00 UTC.

Time history pressure drops obtained from the “wind radii treatment” are compared with those of Best Track data sets for Earl (Figure 10) and Nargis (Figure 11). The red line represents pressure drop from the wind radii treatment, while the blue line those from the Best Track data sets. Instead the green line represents for Earl the pressure drop provided in the Advisories data (this parameter is provided in Atlantic Basin), while for Nargis the pressure drop provided in JTWC best track data.

The pressure drops obtained for TC Earl are consistent with the NOAA Best Track data and advisory data before the advisory 34 (2 September 2010 21 UTC). After this date there are high differences. The reasons of these differences are still under evaluation. For TC Nargis, the wind radii treatment results are consistent with those of JTWC, while there is a big difference with those of RSMC data. The minimum JTWC’s Pc is 937 mbar, while that of RSMC is 962 mbar (Kuroda et al., 2010). The RSMC uses 10-min averaged wind, while JTWC uses 1-min. This could be one of the reasons of this difference between the RSMC and JTWC data.

Concluding the pressure drop profile obtained from the wind radii treatment is consistent with the values provided by the Best Track data. Therefore the obtained Holland’s parameters will be used to infer the atmospheric forcing – wind and pressure fields – for the *HyFlux2* storm surge simulations. This method can be applied in all TC basins because it is using the world available wind radii data provided in each TC bulletin.

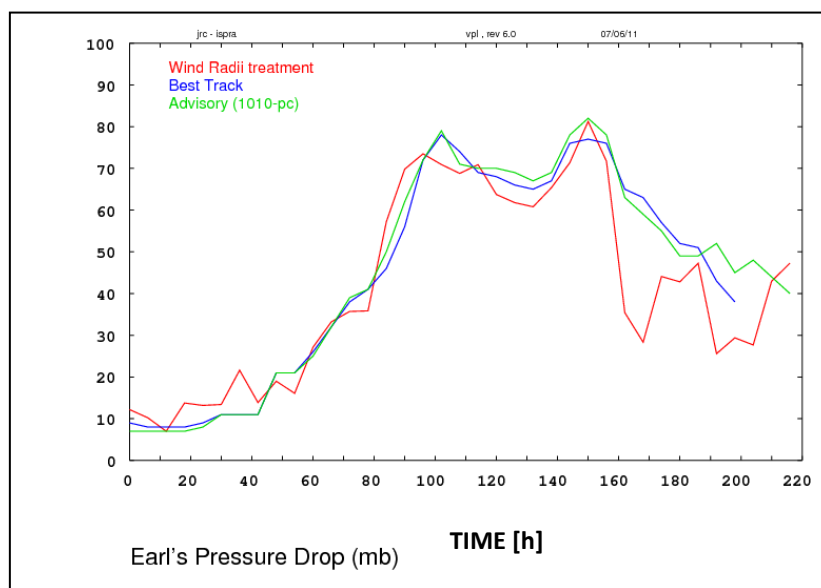


Figure 10 - Earl Pressure Drop (time 0 = 27 August 2010 03:00 UTC).

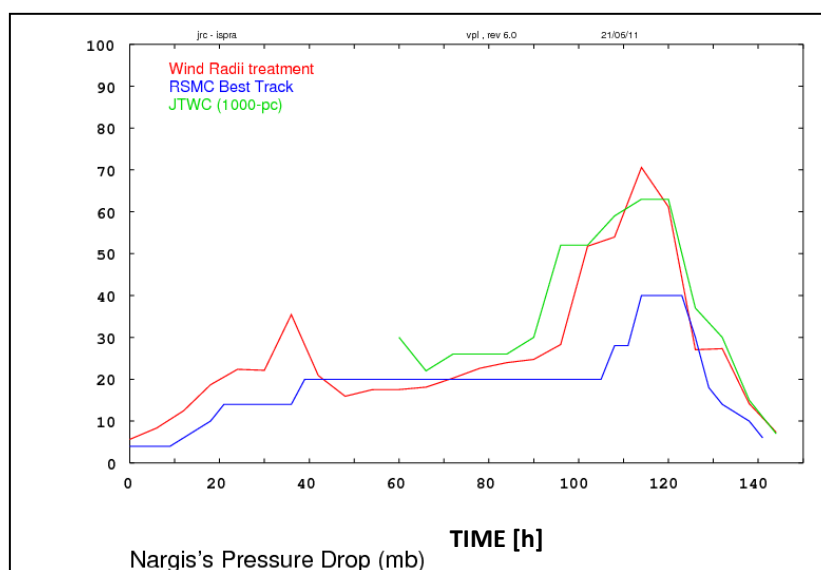


Figure 11 - Nargis's Pressure Drop (time 0 = 27 April 2008 12:00 UTC).

4. STORM SURGE SIMULATIONS

The Holland's parameters are obtained from the wind radii treatment of three different TCs: Katrina, Nargis and Yasi. For Katrina, the NOAA Best Track data are used as input for the wind radii treatment, while for Nargis and Yasi the bulletins advisories (time 0) available in GDACS data base are used. Therefore the obtained Holland's parameters are used to infer the atmospheric forcing – wind and pressure fields – for the HyFlux2 storm surge simulations. The final results of the hydrodynamic simulations are the inundation maps (the area affected by flood), and the maximum water height in the coastline. The simulations are performed in two steps: a first simulation is done on a large area, adopting a grid size of 2min (about 3600m) and then a nested simulation with a 0.25min grid size is performed, allowing to identify the inundated areas with more detail. The simulations are performed from the first time when the TC is advised to fall in the land.

4.1. KATRINA (23-30 August 2005)

Katrina was one of the most damaging TCs disasters in the history of the United States, causing fatalities and damage in several regions (southern Florida, Gulf of Mexico, Louisiana and Mississippi, Florida panhandle, Georgia and Alabama). At least 1836 people died, the most significant amount of deaths occurred in New Orleans, Louisiana.

Katrina formed over the Bahamas on August 23 and crossed southern Florida (first landfall) as a moderate Category 1 hurricane on Saffir-Simpson Scale (Appendix B), causing deaths and flooding. After Katrina moved westward, entering in the Gulf of Mexico, and began strengthening rapidly, reaching Category 5 on Saffir-Simpson Scale, with a maximum wind of 150 kts and a minimum of pressure of 902 mbar. After the hurricane weakened to Category 3 and on August 29 it made the second (near Buras, Louisiana) and third landfall (near Louisiana/Mississippi border) on the northern Gulf coast. Strong winds and an elevated pressure drop created an extreme storm surge, causing fatalities and damage. Most of the damage had due to a secondary effect of this surge: the surge caused a rise of the level of Lake Pontchartrain, straining the levee system protecting New Orleans, and on August 30 significant failures in this system occurred, pouring water into the city which sits mostly below sea level. After creating death and destruction in Louisiana, Mississippi, and Alabama, Katrina moved northward into Tennessee and Kentucky and points northeast from there, dissipating on August 30. In Figure 12 Katrina's track is shown.

More information can be found in Knabb et al. (2005) and in Graumann et al. (2006).



Figure 12 - Katrina's track (Source http://en.wikipedia.org/wiki/File:Katrina_2005_track.png).

The pressure field obtained using the wind radii treatment and the Holland's model is shown in Figure 14, while the wind field is in Figure 15. These figures show the intensity and the track of Katrina. In Figure 15 three of the thresholds used to represent the buffer of wind correspond to the values of the wind radii data 64, 50 and 34 knots. Two others threshold are used to shown the area affected by winds lower than 18 m/s. In Figure 12 the intensity of Katrina is shown using the Saffir-Simpson Scale described in Appendix B. Katrina reached Category 1 over the South of Florida. The velocity of winds of Category 1 is between 33 and 42 m/s. In our wind map a value higher than 33 m/s has been found after crossing this area. Two examples of Katrina wind

analysis obtained using wind radii method and Holland’s model, for 29 August 2005 (12 UTC) and 29 August 2005 (12 UTC), are presented in Figure 13. In these figures the wind speed counters are in knots. Figure 13 (left) shows the wind field of Katrina when it was a hurricane of Category 5, with very strong winds (with a maximum of 136 knots), while Figure 13 (right) shows the wind field before the landfall in Louisiana. A complete reconstruction of Katrina wind field can be found in Powell et al. (2010).

The atmospheric forcing obtained is then used in HyFlux2 to simulate the inundation area. In Figure 17 the inundation map (0.25 min grid size) of the most inundated area (Gulf of Mexico) is shown. NOAA inundation map - a post-storm Landsat satellite imagery - of the same area is presented in Figure 16. The inundation area simulated by the hydrodynamic model is consistent with the observations. A difference can be found in the area of New Orleans, because the satellite image capture also the flood due to the problems at the levee system, while in the simulation these infrastructure have not been considered.

Also the maximum heights simulated by HyFlux2 are consistent with the observations. A maximum height of 7.22 m is simulated in the region of Pass Christian and a value of 8.4 m has been observed in this area (Graumann et al., 2006). A complete storm surge analysis is presented in NOAA storm surge report⁶. The observed data shown in this article are compared with the HyFlux2 simulations. The results of this comparison, for the area most inundated, are presented in Table 6. The difference between the simulations and the observations are less than 1m for five cases, while for two is more than 2 m. The reasons of these differences are under evaluation.

The rainfall amounts from Katrina, though rather high in some places, were not the main impact of this storm, therefore are not evaluated in this report.

Station Name	Latitude	Longitude	HyFlux2 MWL (m)	NOAA MWL (m)	Difference
Dauphin Island , AL	30.25	-88.075	1.564	1.942	-0.378
Horn Island, MS	30.23833	-88.6667	2.876	1.898	0.978
Ocean Springs, MS	30.39167	-88.7983	4.075	4.043	0.032
Biloxi, MS	30.41167	-88.9033	4.376	1.316	3.060
Waveland, MS	30.28167	-88.3667	2.068	2.737	-0.669
East Bank, LaBranche, LA	30.05	-90.3517	2.154	1.865	0.289
Grand Isle, LA	30.26333	-88.9567	4.072	1.739	2.333

Table 6 - NOAA Maximum water levels (MWL) for Katrina compared with those simulated by HyFlux2.

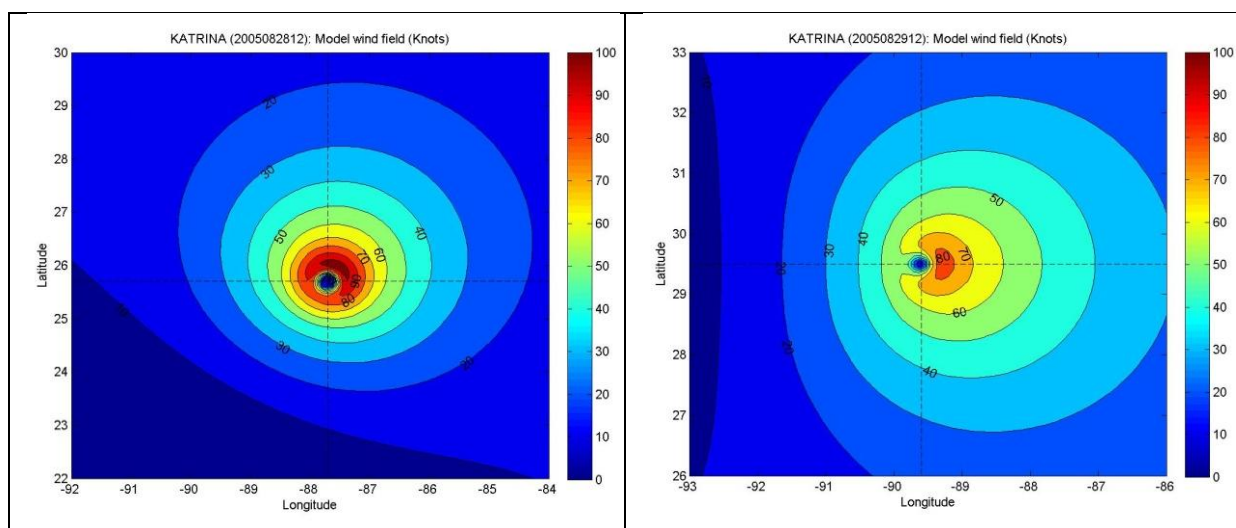


Figure 13 – Katrina’s wind field obtained using the Holland’s model and wind radii treatment for: (left) 28 August 2005 (12 UTC) and (right) 29 August 2005 (12 UTC).

⁶ <http://tidesandcurrents.noaa.gov/publications/HurricaneKatrina2005PreliminaryWaterLevelsReport.pdf>

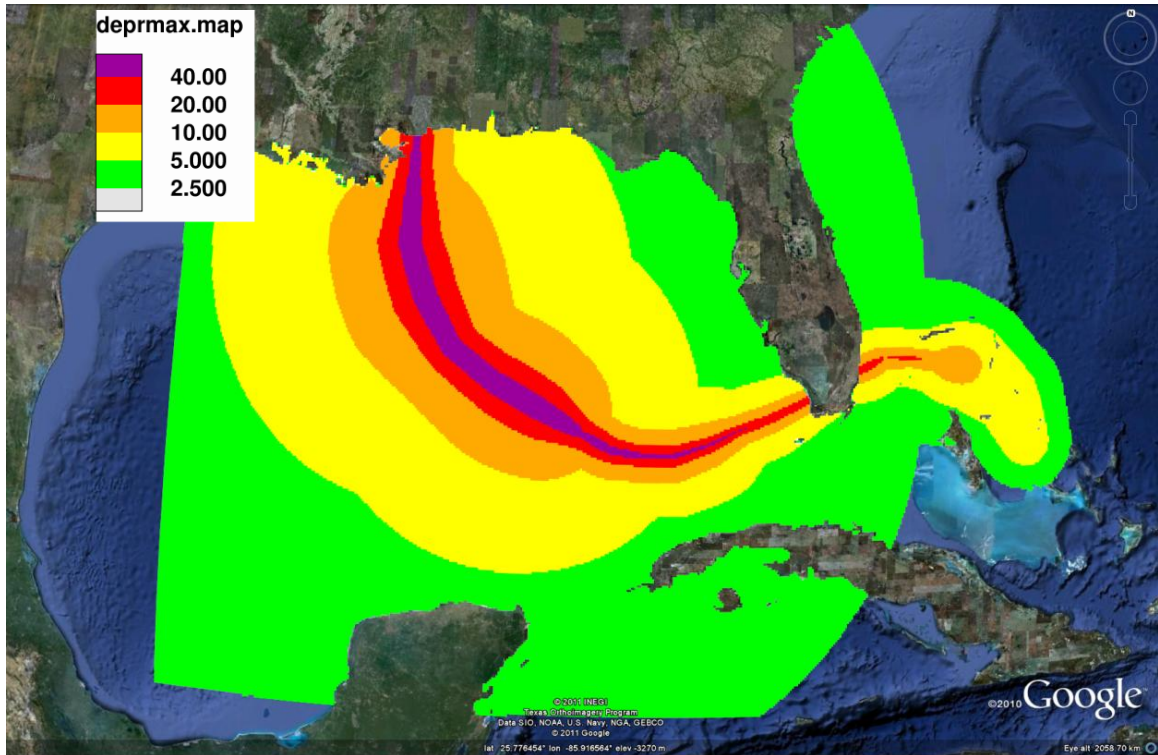


Figure 14 - Katrina's maximum pressure fields expressed in mbar, obtained using the wind radii treatment and the Holland's model

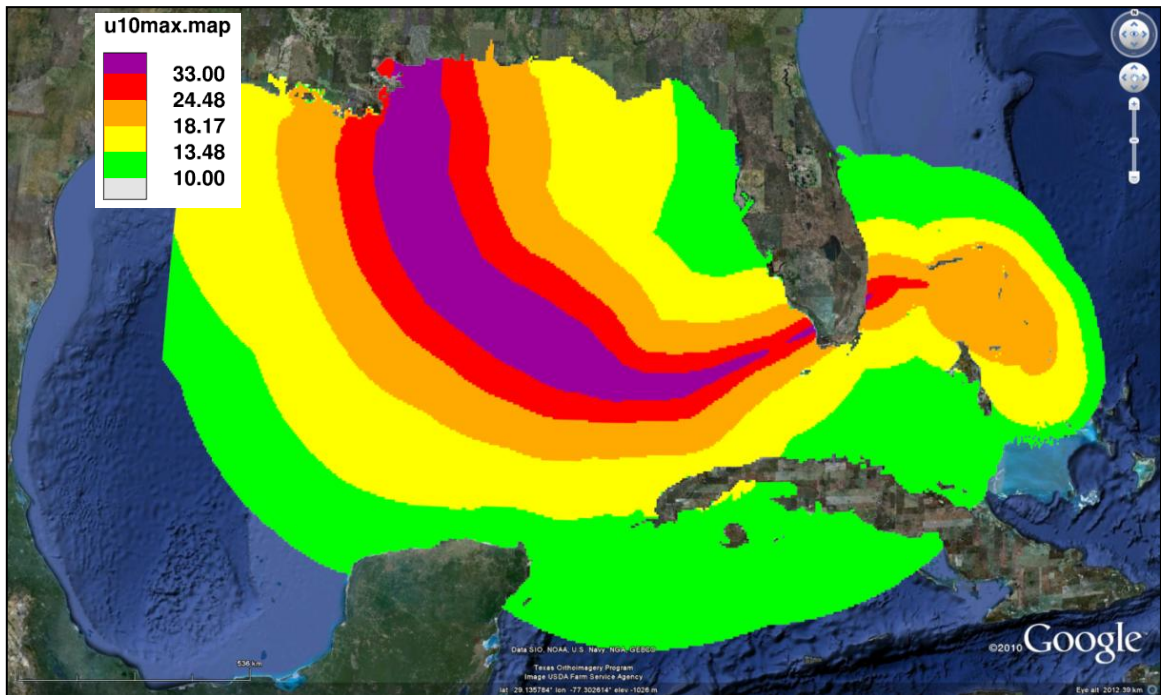


Figure 15 - Katrina's maximum wind field expressed in m/s, obtained using the wind radii treatment and the Holland's model

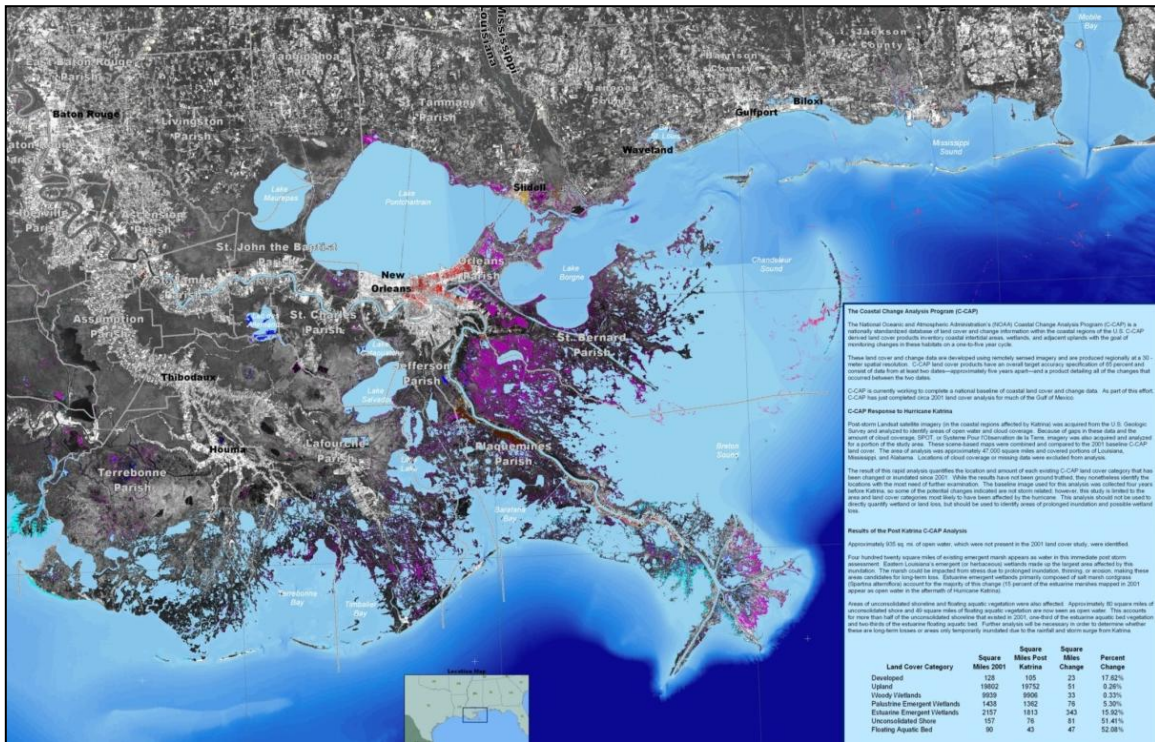


Figure 16 - Katrina's inundation map detected by NOAA.
 (Source: <http://www.katrina.noaa.gov/maps/images/katrina-coastal-inundation-gulf-coast2.jpg>)

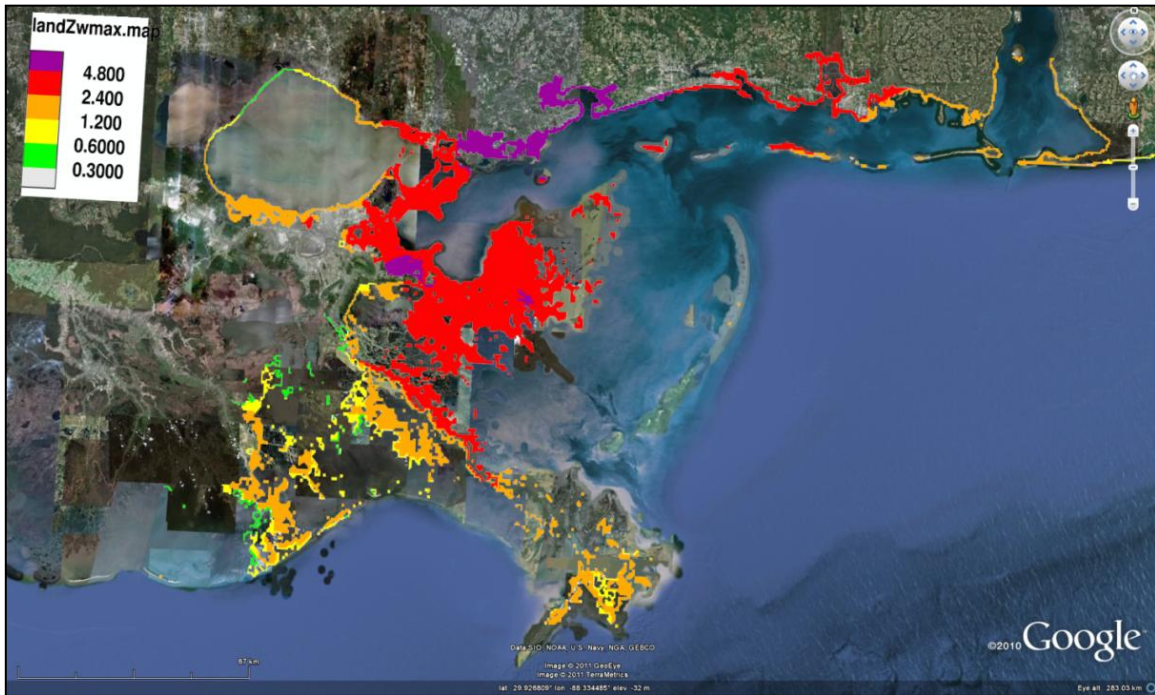


Figure 17 - Katrina's inundation map obtained using HyFlux2.

4.2. NARGIS (27 April – 3 May 2008)

TC Nargis, known as the “Myanmar Cyclone”, was a strong TC occurred in 2008 that caused the worst natural disaster in the recorded history of Myanmar, killing in this region more than 22’000 people according to Tyagi et al. (2008), while 84’000 people died according to RSMC (2009).

A low pressure has been created in the morning of 26 April 2008, than under favorable atmospheric condition (e.g. warmer sea surface temperature) became a tropical depression on 27 April. Initially it moved westwards, increasing its intensity, and became a cyclone of Category 1. Then it moved eastward increasing its intensity until become a very severe cyclone⁷ before landfall in Myanmar on 2 May. Between 12 and 14 UTC of 2 May it crossed the southwest coast of Myanmar, causing a destructive damage during its passage; then moved inland to the northeast and rapidly decayed as a low pressure area over northeast of Myanmar and adjoining Thailand on 3 May 2008.

Nargis had very strong winds, the maximum wind speed exceeded 40 m/s. These extremes winds caused a destructive storm surge flooding in low land coastal area, that it is responsible of most of the fatalities in the affected area. A storm surge of about 3-5 meters over the Ayeyarwady delta region of Myanmar has been reported in (RSMC, 2009).

Details of Nargis’s damage are given in Table 7, while more information can be found in RSMC (2009), Tyagi et al. (2010) and Kuroda et al. (2010).

Damage of TC Nargis	
Affected population	11 millions
Houses Damaged	745764
Deaths (human)	84000
Missing (human)	54000
Injured people	20000

Table 7 - Damage of TC Nargis. Source: RSMC (2009).

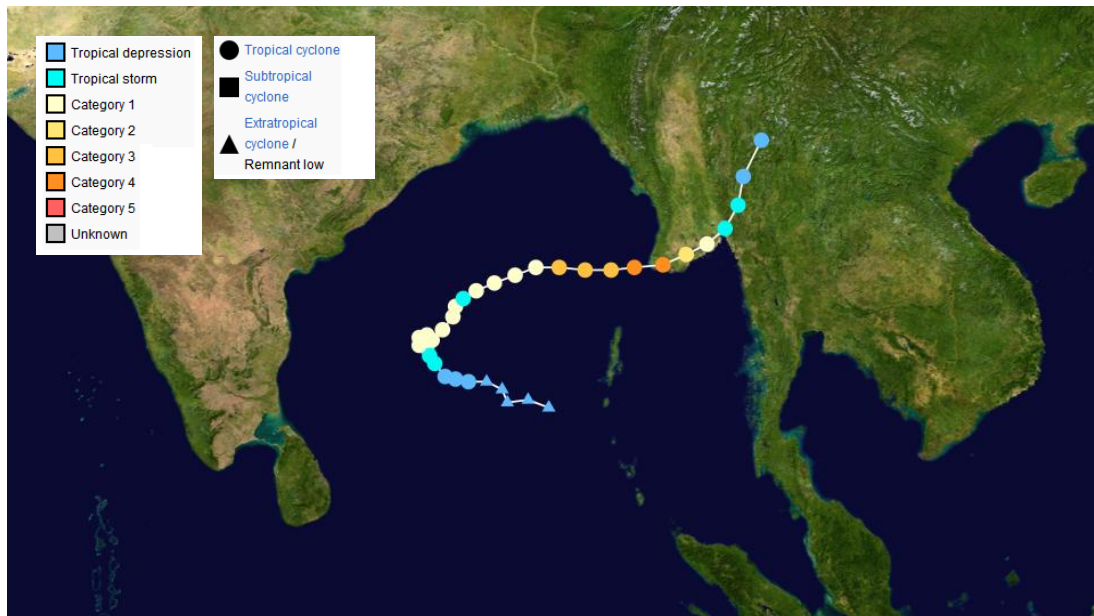


Figure 18 – Nargis’s track.

(Source: http://upload.wikimedia.org/wikipedia/commons/0/03/Nargis_2008_track.png)

The pressure field obtained using the Holland’s method is shown in Figure 19, while the wind field is presented in Figure 20. These figures show that Nargis developed on the Bay of Bengal as a tropical storm (first bulletin on 27 April 2008). The wind velocities, when Nargis developed, are between 18 and 33 m/s (orange-red areas in Figure 20), while the pressure are between 10 and 25 mbar (yellow-red color in Figure 19).

⁷Based on the RSMC New Delhi scale which corresponds to Category 4 of the US. Saffir-Simpson Scale.

After 29 April Nargis moved eastward, increasing the intensity of wind and pressure drop, making landfall in Myanmar on 2 May 2008. In Figure 19 the maximum pressure drop, before landfall is more than 40 mbar (purple area). RSMC New Delhi estimated a pressure drop of 40 mbar, while the JTWC of 60 mbar (Figure 11). The wind, before landfall, had a velocity more than 33 m/s (purple area). These intense pressure and wind fields (atmospheric forcing) created a storm surge in the Ayeyarwady delta region of Myanmar. The inundation map simulated by HyFlux2 of this area is shown in Figure 22, while the inundated area observed by satellite (UNOSAT map) is shown in Figure 21. The comparison of this two maps, point out that the inundated area simulated by the hydrodynamic model is lower than that observed by the satellite. The rainfall effect could be one of the reasons of these differences. Nargis rainfall has been very heavy, a time series of rainfall over southern Burma and the Andaman Sea indicated almost 600 mm of rainfall in some areas⁸. The total rainfall from 27 April to 4 May 2008 of the NASA near-real time Multi-satellite Precipitation Analysis are shown in relation to Nargis' track in Figure 23.

The rainfall effect can influence also the value of maximum water height. The maximum heights simulated by HyFlux2 are consistent with the values shown in Tyagi et al. (2010) for the Irrawaddy delta region, with a value of about 3.6 m for this area (red area in Figure 22). A storm surge of about 3-5 meters over the Ayeyarwady delta region has been reported in RSMC (2009). Same values have been simulated by HyFlux2 in this area. In RSMC (2009), the storm surge heights estimated by Department of Meteorology and Hydrology of Myanmar are presented. The results of this analysis are compared with the HyFlux2 simulations and are presented in Table 8. In this Table the HyFlux2 simulations are also compared with the observed data provided in Lin et al. (2010) and the value of a GLOSS Tide Gauge (Mulein Station). In all comparisons, except for Magyibin, the maximum heights simulated by HyFlux2 are lower than the observed data. This could be due to the rainfall effect not included in the hydrodynamic model. For Thetkethaung and Apoung the difference is more than 4 m, but the value of Apoung disagrees with the value provided in Lin et al. (2010) and comparing the HyFlux2 simulation with this data, the difference is 1.34 m and not 5.05 m. The last comparison, with the data of Mulein Station (GLOSS Tide Gauge), shows a close agreement with the HyFlux2 simulation: a difference of only 0.29 m is found.

Actually no more data have been found for a complete validation, because in Myanmar few observed data are available. Nevertheless these comparisons have shown that an additional effort must be done in order to include the rainfall effect in HyFlux2 code.

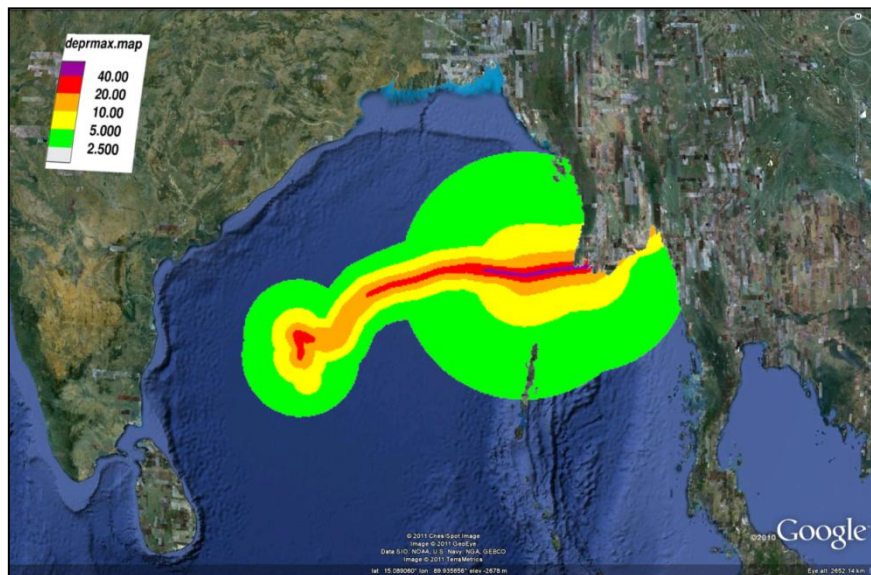


Figure 19 – Maximum Pressure field of Nargis, obtained using the wind radii treatment and the Holland's model

⁸ http://www.nasa.gov/mission_pages/hurricanes/archives/2008/h2008_nargis.html

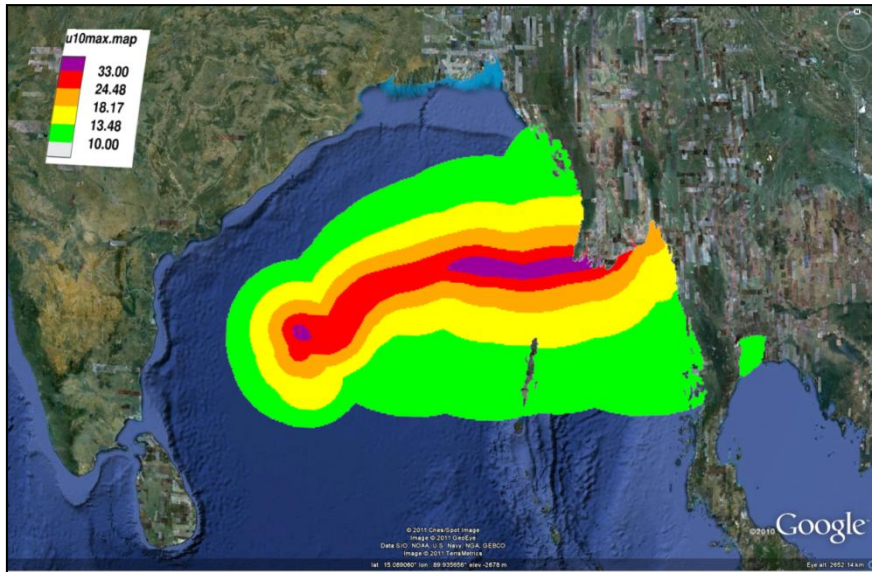


Figure 20 - Maximum Wind field of Nargis, obtained using the wind radii treatment and the Holland's model

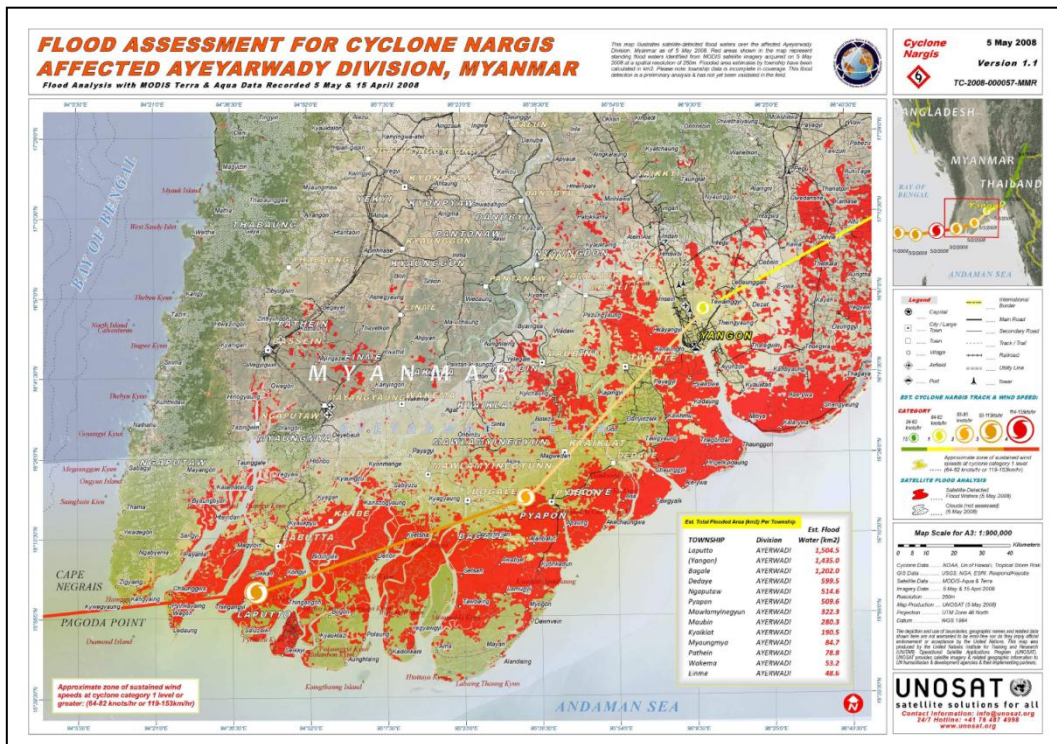


Figure 21 - UNOSAT map of the flood assesment for Nargis. (source <http://www.unitar.org/unosat/maps/MMR>)

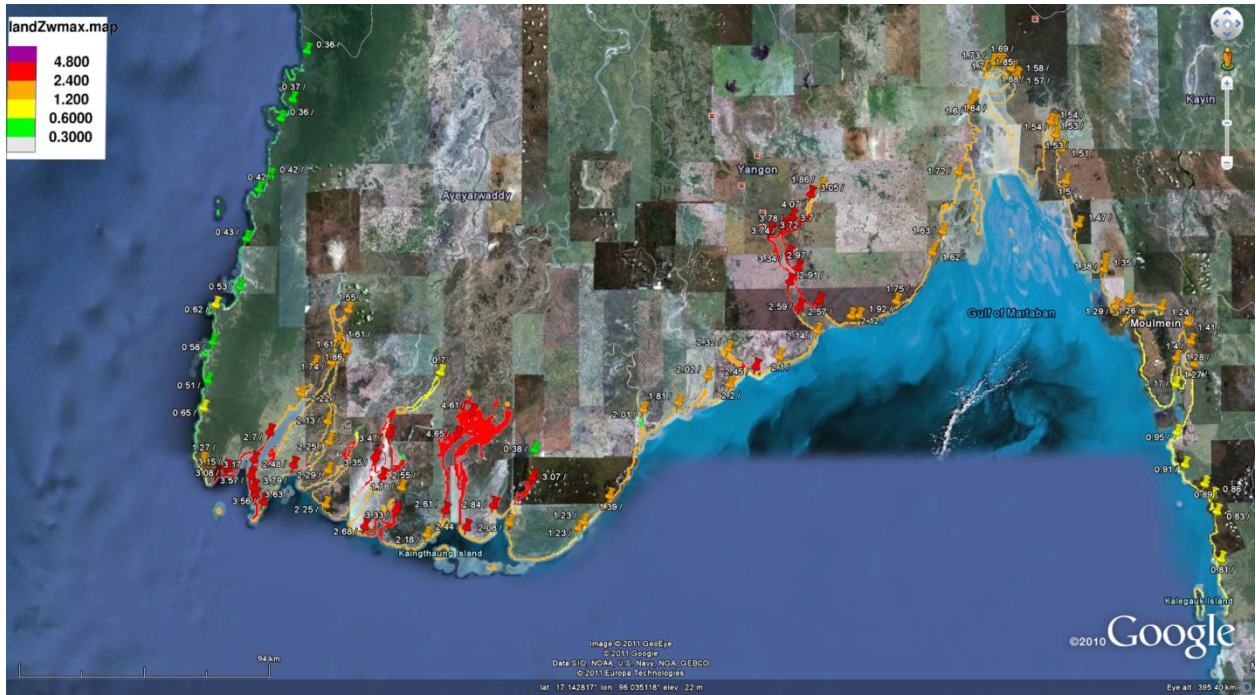


Figure 22 - Inundation map of Nargis simulated by HyFlux2.

Location	Latitude	Longitude	HyFlux2 MWL (m)	Observed/ Analyzed MWL (m)	Difference
Kangyaing ⁽¹⁾	15.9656	94.2625	2.64	4.57	- 1.93
Thetkethaung ⁽¹⁾	15.9941	94.5281	2.02	6.40	-4.38
Magyibin ⁽¹⁾	16.1381	94.6458	1.77	1.52	0.25
Apoung ⁽¹⁾	16.1771	95.7292	1.66	6.71	-5.05
Phyapon (Apaung) ⁽²⁾	16.1771	95.7292	1.66	3.00	-1.34
Laputta (Bidutgale) ⁽²⁾	16.0993	94.861	3.02	3.35	-0.33
Thingangyi ⁽²⁾	16.2	95.85	2.02	3.20	-1.18
Chaunggwa ⁽²⁾	16.0104	94.3917	2.68	4.95	-2.27
Moulmein Station ⁽³⁾	16.4833	97.6166	1.23	1.52	-0.29

Table 8 - Comparisons of inundation heights between HyFlux2 simulations and the analysis of Department of Meteorology and Hydrology - Myanmar (1), the observed data showed in Lin et al. (2010) (2) and the GLOSS tide gauge data of Moulmein station (3).

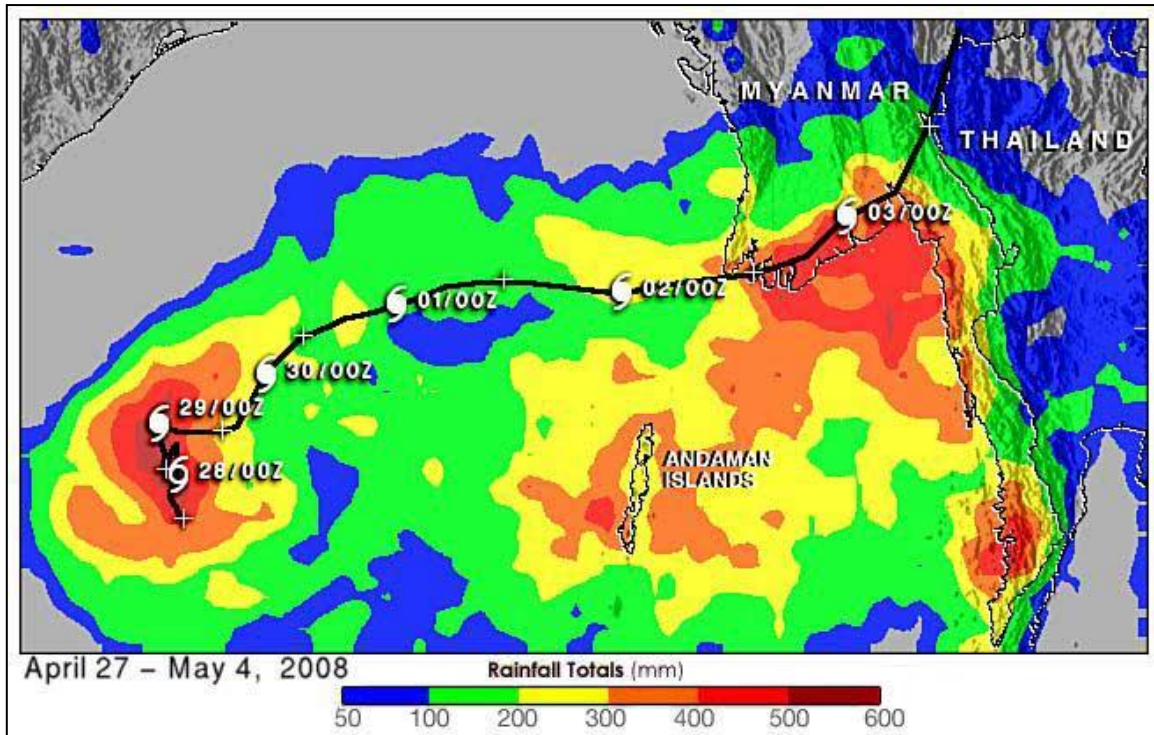


Figure 23 - Total of Rainfall for TC Nargis.

(source: http://www.nasa.gov/images/content/226163main_nargis_rain_27apr4may08.jpg).

4.3. YASI

Cyclone Yasi is a massive TC that caused damage to Queensland, Australia, in 2011. It began developing as a tropical cyclone low northwest of Fiji on January 29 and started tracking on a westward direction. The low pressure quickly intensified to a cyclone category and was called Yasi by Fiji Meteorological Service. Then increase its intensity and began moving west-southwestward, accelerating towards the tropical Queensland coast. The landfall happened on February 2 along the northeast coast of Queensland as a Category 4 on the U.S. Saffir-Simpson scale (Appendix B) midway between Cairns and Townsville. After landfall, it maintained a strong core with damaging winds and heavy rain, tracking westwards across northern Queensland. Finally it weakened to a tropical low near Mount Isa on February 3. Yasi's track is shown in Figure 24.

Actually no observations of the maximum wind near the TC center are available, but the Bureau of Meteorology (BOM) estimated a maximum sustained wind speed of 57 m/s. A minimum pressure of 930 mbar has been recorded by a barograph at the Tully Sugar Mill and by measurements of instrumentation operated by the Queensland Government (Department of Environment and Resource Management) at Clump Point. The pressure measurements taken at Clump Point can be found at <http://www.bom.gov.au/cyclone/history/yasi.shtml>.

Yasi produced a storm surge that hit the north Queensland coast. A 5 m tidal surge was observed at the Department of Environment and Resource Management storm tide gauge at Cardwell, which is 2.3 m above Highest Astronomical Tide (HAT).

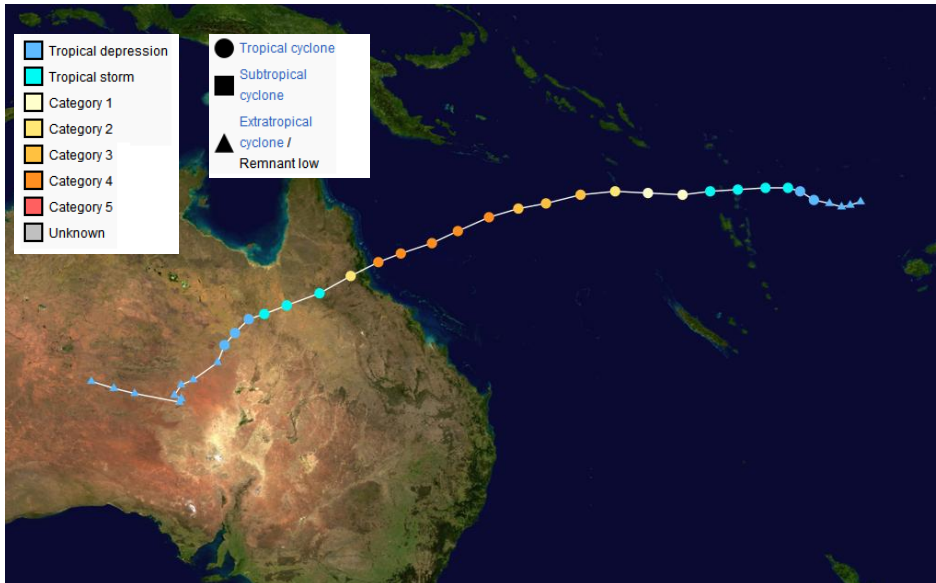


Figure 24 - Yasi's track. (http://en.wikipedia.org/wiki/File:Yasi_2011_track.png)

At the time of writing there are no verified observations of the maximum wind near the TC centre for a complete evaluation of the wind field, only some observation of mean sea level pressure are available, therefore actually no enough observational data are available to a complete assessment of the results of this TC. Below only a preliminary analysis of this recently TC is presented.

In Figure 26 the pressure field obtained using the Holland's model –after wind radii treatment- is presented. A minimum pressure of 930 mbar has been observed near the center of the TC immediately after its landfall (**barograph at the Tully Sugar Mill**), that corresponds to a pressure drop of 80 mbar. Same value is presented in the analysis of the regional weather forecasting model.

In Figure 27 the wind field simulated by our method is presented. Unfortunately no observational data are available to evaluate our results.

The pressure and wind fields are used as input in HyFlux2 to obtain the inundation maps presented in Figure 27. No satellite map are available for a complete assessment of the inundation area. The maximum height simulated by HyFlux2 is 5.99 m in Cardwell, which is consistent with a storm tide of 5 m recorded in this place.

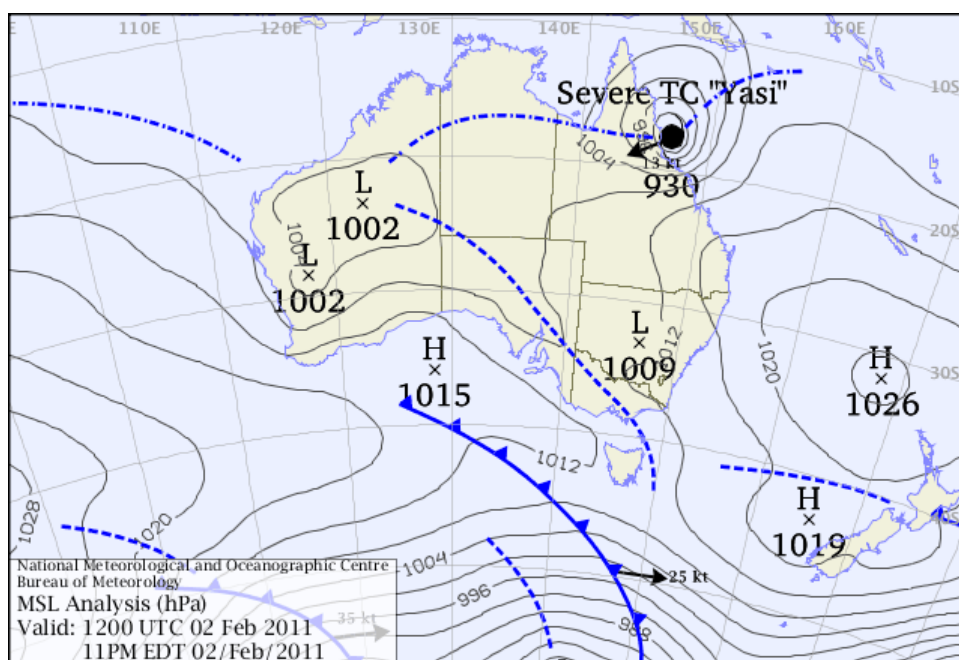


Figure 25 - Analysis for 12:00 on Wednesday UTC 2 February 2011 from Bureau of Meteorology. (<http://www.bom.gov.au/cyclone/history/yasi-mslp.shtml>)

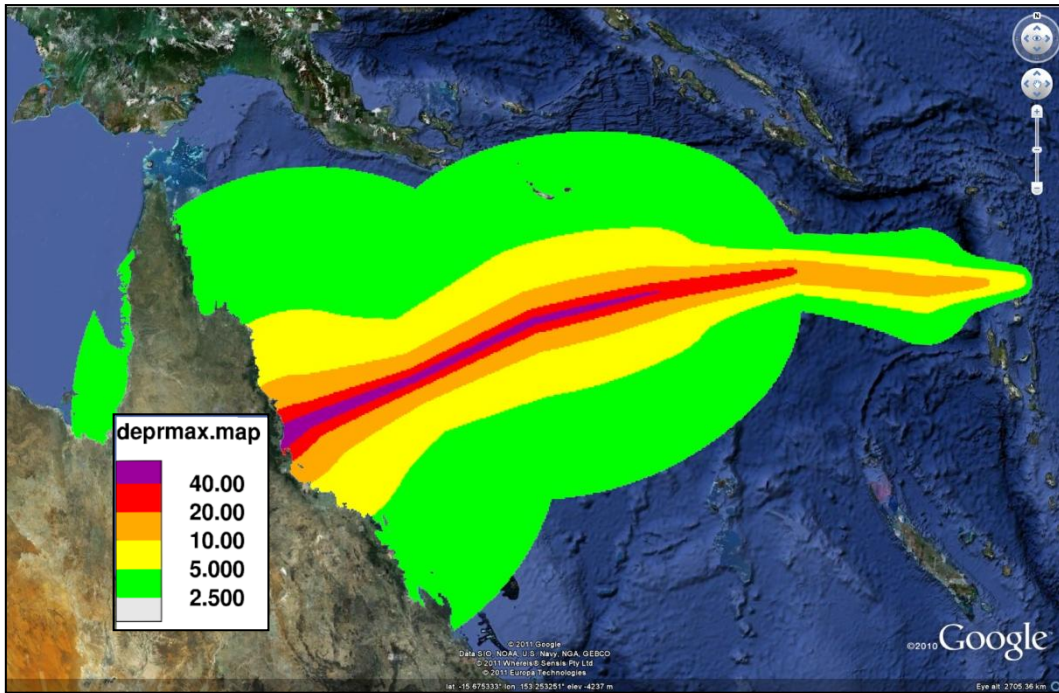


Figure 26 – Yasi's Maximum Pressure field (mbar), obtained using the wind radii treatment and the Holland's model

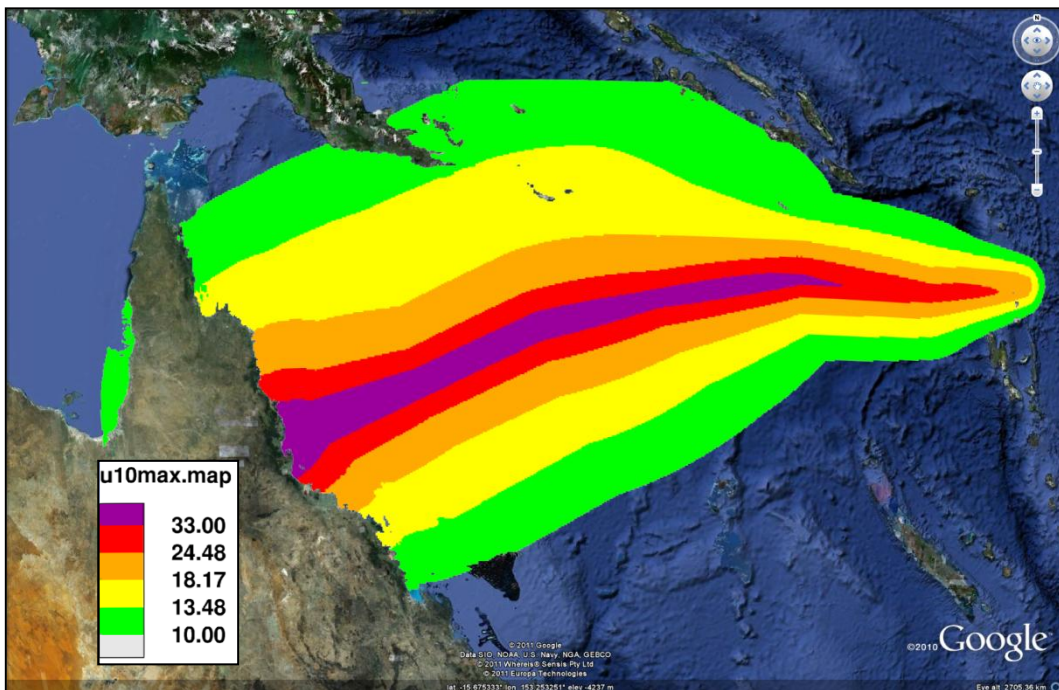


Figure 27 - Yasi's Maximum Wind Field (m/s), obtained using the wind radii treatment and the Holland's model

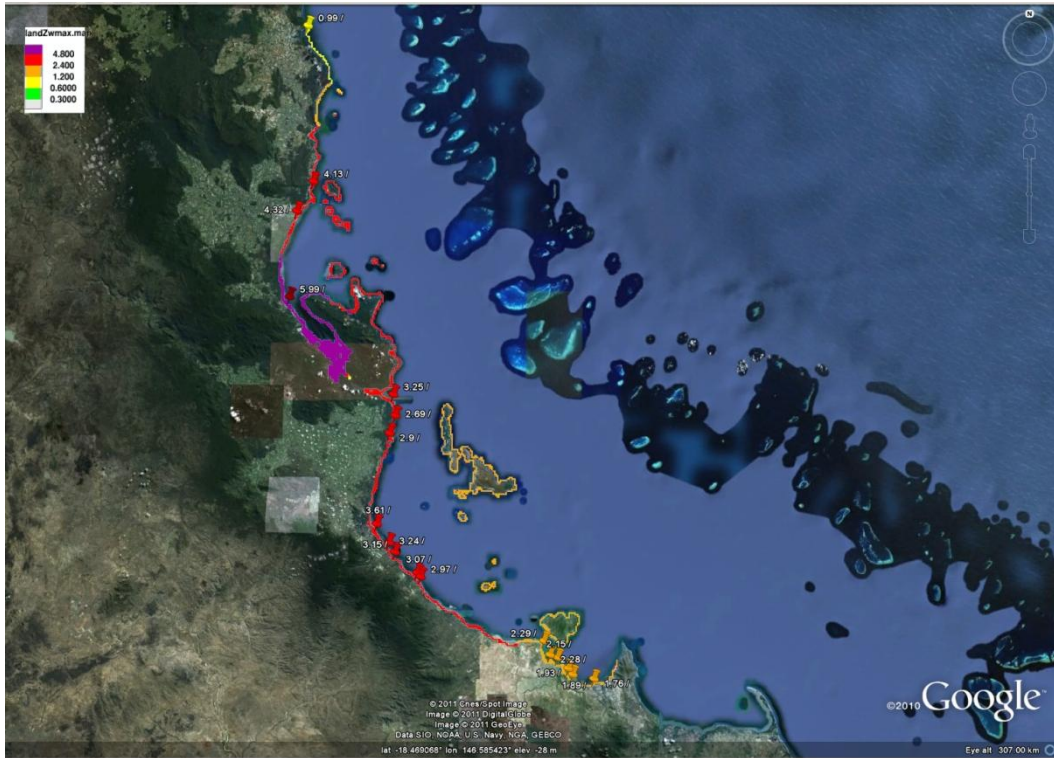


Figure 28 - Inundation map of TC Yasi, obtained using HyFlux2.

5. CONCLUSIONS

The Joint Research Centre (JRC) of the European Commission has developed GDACS, an early warning system developed to alert the humanitarian community about potential disasters which are under an alerting. Tropical cyclones (TCs) are some of the most damaging events. They affect the coastal population through three dangerous effects: strong winds, heavy rains and storm surges. In order to estimate the area and the population affected by a TC, all the three types of physical impacts must be taken into account.

Storm surge is an abnormal rise of water above the normal astronomical tides, generated by strong winds and by a drop in the atmospheric pressure. These atmospheric forcing generates long waves that can be simulated by the shallow water equations. In the last years JRC has developed extensive experience in tsunami early warning system using HyFlux2 model, which solves the shallow water equations by a finite volume method: therefore the JRC has implemented the storm surge phenomena in the Tsunami code, introducing the atmospheric forcing in the shallow water equations.

Accurate surface wind and atmospheric pressure fields are required in storm surge modeling. Therefore the first aim of this work has been to identify which source of information (provided by the different weather forecast center) allows the specification of accurate TC pressure and wind at global level. Several methods exist, the most used in TC modeling are the following: 1) Global or regional weather forecasting model (e.g. GFS, HWRF and GFDL); 2) Parametric model (e.g. Holland's model). The products of the first class of models are not accurate enough, or are not available online at a global scale.

The lack of a global, online, and free downloadable TC datasets, has led the JRC to use the worldwide free available wind radii data to evaluate the Holland's parameters – by a Monte Carlo Method - which are then used to build the wind and pressure fields. The preliminary results obtained from such wind radii treatment are consistent with the available best track data.

The simulation results provided by the hydrodynamic code have been preliminarily validated in TCs occurred in different basins: Katrina in the Atlantic (23-30 August 2005), Nargis in the Indian Ocean (27 April – 3 May 2008) and Yasi in Australia (29 January – 2 February 2011).

For the TC Katrina the storm surge simulated by HyFlux2 is consistent with the observations, except in the New Orleans area, where most of the flood is due to the problems at the levee system, but not to storm surge. Also the results of Yasi agree with the available observations. Instead the results of Nargis differ from the satellite observations, in particular the inundation area simulated by HyFlux2 is smaller than that observed by satellite. The reason of this difference could be due to the additional rainfall effect which was not incorporated into the hydrodynamic code. However, the results are encouraging because the coastline inundation caused by storm surge is captured correctly.

Next step of our work could be to combine in the hydrodynamic model the rainfall - already included in GDACS - with the storm surge effect. The wave hold-up due to the radiation stress is another effect that should be included in the code.

6. REFERENCES

- Alimov, V. V. (2005). Integrated modeling of storm surges during hurricanes Isabel, Charley, and Frances. PhD. University of Florida.
- Atkinson, G. D., and Holliday, C. R. (1977). Tropical cyclone minimum sea level pressure/maximum sustained relationship for the Western North Pacific. *Mon. Wea. Rev.*, 105, 421-427.
- Bender, M., Ginis, I., Tuleya, R., Thomas, B., and Marchok, T. (2007). The operational GFDL coupled hurricane-ocean prediction system and a summary of its performance. *Monthly Weather Review*, 12, 3965-3989.
- Bhowmik, S. K., Kotal, S. D., and Kalsi, S. R. (2005). An Empirical Model for Predicting the Decay of Tropical Cyclone Wind Speed after Landfall over the Indian Region. *J. Appl. Meteor*, 44, 179-185.
- Blain, C., Westerink, J. J., Luettich, R. A., and Scheffner, N. W. (1994). ADCIRC (1994): An advanced three-dimensional circulation model for shelves, coasts, and estuaries. Report 4 Hurricane storm surge modeling using large domains. Washington, DC 20314-1000: US Army Corps of Engineers.
- Bunya, S., Dietrich, J. C., Westerink, J. J., Ebersole, B. A., Smith, J. M., Atkinson, J. H., et al. (2010). A high-resolution coupled riverine flow, tide, wind, wind wave, and storm surge model for southern Louisiana and Mississippi. Part I: Model development and validation. *Mon. Wea. Rev.*, 138, 345-377.
- Campana, K., and Caplan, P. (2005). Technical procedure bulletin for T382 Global Forecast System. Retrieved from NOAA, Environmental Modeling Center, National Centers for Environmental Prediction: http://www.emc.ncep.noaa.gov/gc_wmb/Documentation/TPBoct05/T382.TPB.FINAL.htm
- Cangialosi, J. P. (2011). Tropical Cyclone Report. Hurricane Earl. (AL072010). 25 August - 4 September 2010. Retrieved 2011, from National Hurricane Center: http://www.nhc.noaa.gov/pdf/TCR-AL072010_Earl.pdf
- Cangialosi, J. P., and Franklin, J. L. (2011). 2010 National Hurricane Center Forecast Verification Report. NOAA/NWS/NCEP/National Hurricane Center.
- Cardone, V. J., and Cox, A. T. (2009). Tropical Cyclone Wind Field Forcing for Surge Models: Critical Issues and Sensitivities. *Nat. Haz*, 51, 29-47.
- Cardone, V., Pierson, W., and Ward, E. (1976). Hindcasting the directional spectrum of hurricane generated. 28, 385-394.
- Chow, S. H. (1970). A study of the wind field in the planetary boundary layer of a moving tropical cyclone. MS Thesis. New York University, School of Engineering and Science, New York, NY.
- CIRIA, CUR, and CEFMEF. (2007). Physical site conditions and data collection. In *The Rock Manual*, C683.
- Courtney, J., and Knaff, J. A. (2009). Adapting the Knaff and Zehr wind-pressure relationship for operational use in Tropical Cyclone Warning Centres. *Australian and Meteorological and Oceanographic Journal*(58), 167 - 179.
- Cox, A., Greenwood, J., Cardone, V., and Swail, V. (1995). An interactive objective kinematic analysis system. 4th international workshop on wave hindcasting and forecasting (pp. 109-118). Banff, Alberta: 16-20 October 1995.
- Cruz, A., Krausmann, E., and Franchello, G. (2011). Analysis of tsunami impact scenarios at an oil refinery. 58, 141-162.

- Dietrich, J. C., Bunya, S., Westerink, J. J., Ebersole, B. A., Smith, J. M., Atkinson, J. H., et al. (2010). A High-Resolution Coupled Riverine Flow, Tide, Wind, Wind Wave, and Storm Surge Model for Southern Louisiana and Mississippi. Part II: Synoptic Description and Analysis of Hurricanes Katrina and Rita. *Mon. Wea. Rev.*, 138, 378–404.
- Dube, S., Murty, T., Feyen, J., Harper, B., Bales, J., and Amer, S. (2010). Storm Surge Modeling and Applications in Coastal Areas. In J. Chan, and J. Kepert, *Global Perspectives on Tropical Cyclones: From Science to Mitigation* (pp. 363-406). World Scientific Publishing Company.
- Franchello, G. (2008). Modelling shallow water flows by a High Resolution Riemann Solver. EUR 23307 EN - 2008, ISSN 1018-5593.
- Franchello, G. (2010). Shoreline tracking and implicit source terms for a well balanced inundation model. *International Journal for Numerical Methods in Fluids*, 63(10), 1123–1146.
- Franchello, G., and Krausmann, E. (2008). HyFlux2: a numerical model for the impact assessment of severe inundation scenario to chemical facilities and downstream environment. EUR 23354 EN – 2008, ISSN 1018-5593.
- Fujita, T. (1952). Pressure Distribution Within Typhoon. *Geophys. Mag.*, 23, 437-451.
- Glahn, B., Taylor, A., Kurkowski, N., and Shaffer, W. (2009). The role of the SLOSH model in National Weather Service storm surge forecasting. *Natl. Wea. Dig.* 1-14.
- Graumann, A., and (US), N. C. (2006). Hurricane Katrina: a climatological perspective: preliminary report. Retrieved from NOAA NCDC: www.ncdc.noaa.gov/oa/reports/tech-report-200501z.pdf
- Hamill, T. M., Whitaker, J. S., Kleist, D. T., Fiorino, M., and Benjamin, G. (2011). Prediction of 2010's tropical cyclones using the GFS and ensemble-based data assimilation methods. Submitted as an "expedited contribution" to *Monthly Weather Review*.
- Harper, B. (2002). Tropical Cyclone Parameter Estimation in the Australian Region: Wind-Pressure Relationships and Related Issues for Engineering Planning and Design. A Discussion Paper. Systems Engineering Australia Pty Ltd, J0106-PR003E.
- Harper, B. A., Kepert, J. D., and Ginger, J. D. (2010). Guidelines for converting between various wind averaging periods in tropical cyclone conditions. World Meteorological Organization, TCP Sub-Project Report, WMO/TD-No. 1555.
- Harper, B., Hardy, T., Mason, L., Bode, L., Young, I., and Nielsen, P. (2001). Queensland climate change and community vulnerability to tropical cyclones, ocean hazards assessment. Stage 1 report. Department of Natural Resources and Mines, Queensland, Brisbane, Australia.
- Heming, J., and Goerss, J. (2010). Track and Structure Forecasts of Tropical Cyclones. In J. Chan, and J. Kepert, *Global Perspectives on Tropical Cyclones: From Science to Mitigation* (pp. 287-323). World Scientific Publishing Company.
- Higaki, M., and Hayashibara, H. (2008). Operational Storm Surge forecasting at Japan Meteorological Agency. Retrieved 2011, from JMA: http://boram.lee.f.free.fr/SSS/full_papers/2_OSS_Higaki_Masakazu.pdf
- Higaki, M., Hayashibara, H., and Nozaki, F. (2009). 25-38. Retrieved 2011, from JMA, Technical Review, No. 11: <http://www.jma.go.jp/jma/jma-eng/jma-center/rsmc-hp-pub-eg/techrev/text11.pdf>
- Holland, G. (1980). An analytical model of the wind and pressure profiles in hurricanes. *Mon. Wea. Rev.*, 108, 1212-1218.
- Holland, G. (2008). A Revised Hurricane Pressure–Wind Model. *Mon. Wea. Rev.*, 136, 3432-3445.

- Holland, G., Belanger, J. I., and Fritz, A. (2010). Revised Model for Radial Profiles of Hurricane Winds. *Monthly Weather Review*, 4393-4401.
- Holton, J. R. (2004). *An Introduction to Dynamic Meteorology*. Elsevier Academic Press.
- Jakobsen, F., and Madsen, H. (2004). Comparison and further development of parametric tropical cyclone models for storm surge modelling. *J. Wind Eng. Ind. Aerodyn*, 92, 375–391.
- Jelesnianski, C. P., Chen, J., and Shaffer, W. A. (1992). *SLOSH: Sea, Lake, and Overland Surges from Hurricanes*. Silver Spring, MD: National Weather Service.
- Kaplan, J., and DeMaria, M. (1995). A simple empirical model for predicting the decay of tropical cyclone wind speed after landfall. *J. Appl. Meteor*, 34, 2499–2512.
- Kieu, C. Q., Chen, H., and Zhang, D. (2010). An Examination of the Pressure–Wind Relationship for Intense Tropical Cyclones. *Wea. Forecasting*, 25, 895–907.
- Knabb, R., Rhome, J., and Brown, D. (2005). Tropical cyclone report: Hurricane Katrina, 23-30 August 2005, National Hurricane Center. NHC report.
- Knaff, J. A., and Zehr, R. M. (2007). Reexamination of the tropical cyclone wind-pressure relationships. *Wea. Forecasting*, 71-88.
- Knaff, J. A., Harper, B. A., Brown, D., Langlade, S., Courtney, J., Herndon, D., et al. (2010). Tropical Cyclone Surface Wind Structure and Wind-Pressure Relationships. Seventh International Workshop on Tropical Cyclones, (pp. KN1.1-KN1.35).
- Knaff, J. A., Sampson, C. R., DeMaria, M., Marchok, T. P., Gross, J. M., and McAdie, C. J. (2007). Statistical tropical cyclone wind radii prediction using climatology and persistence. *Wea. Forecasting*, 22, 781–791.
- Knapp, K. R., Kruk, M. C., Levinson, D. H., Diamond, H. J., and Neumann, C. J. (2010). International Best Track Archive for Climate Stewardship (IBTrACS): Unifying tropical cyclone best track data. *Bull. Amer. Meteor. Soc.*, 91, 363-376.
- Kurihara, Y., Tuleya, R., and Bender, M. (1998). The GFDL hurricane prediction system and its performance in the 1995 hurricane season. *Mon. Weather Rev.*, 126 (5), 1306-1322.
- Kuroda, T., Saito, K., Kunii, M., and Kohno, N. (2010). Numerical simulations of Myanmar cyclone Nargis and the associated storm surge Part I: Forecast experiment with a nonhydrostatic model and simulation of storm surge. *Journal of the Meteorological Society of Japan*, 88, 521-545.
- Leuttich, R. J., Westerink, J., and Scheffner, N. (1992). ADCIRC: an advanced three-dimensional circulation model for shelves, coasts, and estuarine. I: theory and methodology of ADCIRC-2DDI and ADCIRC-3DL. *DRP Tech. Rep. 1*. Waterways Experiment Station, Vicksburg, MS: US Army Corps of Engineers.
- Lin, N. M., and Sayama, T. (2010). Storm surge inundation analysis of cyclone Nargis event. Retrieved 2011, from ICHARM: www.icharm.pwri.go.jp/training/master/publication/pdf/2010/nay.pdf
- Melton, G., Gall, M., Mitchell, J. T., and Cutter, S. L. (2009). Hurricane Katrina storm surge delineation: implications for future storm surge forecasts and warnings. *Nat Hazards*, 54, 519-536.
- Miller, M. (2010). Development of the deterministic system. Forecast Products Users' Meeting, 9-11 June 2010. ECMWF.

- Niedoroda, A. W., Resio, D. T., Toro, G. R., Divoky, D., Das, H. S., and Reed, C. W. (2010). Analysis of the coastal Mississippi storm surge hazard. *Ocean Engineering*, 37, 82–90.
- Powell, M. D. (1980). Evaluations of diagnostic marine boundary layer models applied to hurricanes. *Mon. Wea. Rev.*, 108, 757–766.
- Powell, M. D., and Houston, S. H. (1996). Hurricane Andrew's landfall in South Florida. Part II: surface wind fields and potential real-time applications. *Weather Forecast*, 11, 329–349.
- Powell, M. D., Houston, S. H., and Reinhold, T. A. (1996). Hurricane Andrew's landfall in South Florida. Part I: standardizing measurements for documentation of surface windfields. *Weather Forecast*, 11, 304–328.
- Powell, M. D., Murillo, S., Dodge, P., Uhlhorn, E., Gamache, J., Cardone, V., et al. (2010). Reconstruction of Hurricane Katrina's wind fields for storm surge and wave hindcasting. *Ocean Engineering*, 37, 26-36.
- Pugh, D. (2004). *Changing sea levels: effects of tides, weather, and climate*. Cambridge Univ Pr.
- Rappaport, E. N., Franklin, J. L., Avila, L. A., Baig, S. R., Beven, J. L., Blake, E. S., et al. (2009). Advances and Challenges at the National Hurricane Center. *Weather and Forecasting*, 24, 395-419.
- RSMC. (2009). Report on cyclonic disturbances over North Indian Ocean during 2008. RSMC, New Delhi.
- Saito, K., T. Fujita, Y. Yamada, J. Ishida, Y. Kumagai, K. Aranami, S. Ohmori, R. Nagasawa, S. Kumagai, C. Muroi, T. Kato, H. Eito and Y. Yamazaki (2006). The operational JMA nonhydrostatic mesoscale model. *Mon. Wea. Rev.*, 134, 1266-1298.
- Schloemer, R. W. (1954). Analysis and synthesis of hurricane wind patterns over Lake Okeechobc, Florida. U.S. Weather Bureau, Department of Commerce and U.S. Army Corps of Engineers. Washington, DC: Hydrometeorological Report. 31.
- Shapiro, L. J. (1983). The asymmetric boundary layerflow under a translating hurricane. *J. Atmos. Sci.*, 40, 1984-1998.
- Shea, D. J., and Gray, W. M. (1973). The hurricanes' inner core region: symmetric and asymmetric structure. *J. Atmos. Sci.*, 30, 1544-1564.
- Sobey, R. J., Harper, B. A., and Stark, K. P. (1977). Numerical simulation of tropical cyclone storm surge along the Queensland Coast. Research Bulletin CS14. Department of Civil and Systems Engineer, James Cook University.
- Surgi, N., Pan, H., and Lord, S. J. (1998). Improvement of the NCEP Global Model over the Tropics: An Evaluation of Model Performance during the 1995 Hurricane Season. *Mon. Wea. Rev.*, 126, 1287–1305.
- Tang, Y. M., Holloway, P., and Grimshaw, R. (1997). A numerical Study of the Storm Surge Generated by Tropical Cyclone Jane. *Journal of Physical Oceanography*, 27, 963 - 976.
- Thompson, E. F., and Cardone, V. J. (1996). Practical modeling of hurricane surface wind fields. *J. Wtrwy., Port, Coast., and Oc. Engrg.*, 122(4), 195-205.
- Tyagi, A., Mohapatra, M., Bandyopadhyay, B. K., Singh, C., and Kumar, N. (2010). Characteristics of Very Severe Cyclonic Storm “NARGIS” over the Bay of Bengal During 27 April to 3 May 2008. In Y. Charabi, and S. Al-Hatrushi, *Indian Ocean Tropical Cyclones and Climate Change* (pp. 315-325). Springer Verlag.

- Van Der Grijin, G. (2002). Tropical Cyclone forecasting at ECMWF: new products and validation. ECMWF Technical Memorandum(386).
- Vernaccini, L., De Groeve, T., and Gadenz, S. (2007). Humanitarian Impact of Tropical Cyclones. EUR 23083 EN, ISSN 1018-5593.
- Vickery, P. J., and Wadhera, D. (2008). Statistical Models of Holland Pressure Profile Parameter and Radius to Maximum Winds of Hurricanes from Flight-Level Pressure and H*Wind Data. *Journal of Applied Meteorology and Climatology*, 47, 2497-2517.
- Vickery, P. J., Masters, F. J., Powell, M. D., and Washera, D. (2009). Hurricane hazard modeling: The past, present, and future. *Journal of Wind Engineering and Industrial Aerodynamics*, (In Press).
- Vickery, P. J., Skerlj, P. F., Steckley, A. C., and Twisdale, L. A. (2000). Hurricane Wind Field Model for Use in Hurricane Simulations. *Journal of Structural Engineering*, 126, 1203-1221.
- Willoughby, H. E., and Rahn, M. E. (2004). Parametric representation of the Primary Hurricane Vortex. Part I: Observations and Evaluation of the Holland (1980) Model. *Monthly Weather Review*, 132, 3033-3048.
- Xie, L., Bao, S., Pietrafesa, L., Foley, K., and Fuentes, M. (2006). A realtime hurricane surface wind forecasting model: Formulation and verification. *Mon. Wea. Rev.*, 134, 1355–1370.
- Zamora, N., Franchello, G., and Annunziato, A. (2011). 01 April 2007 Solomon Island Tsunami: Case Study to validate JRC Tsunami Codes. EUR 24783 EN - 2011, ISSN 1018-5593.

APPENDIX A: TROPICAL WARNING CENTRES

TCs around the globe are monitored as a result of international cooperation, coordinated at the global and regional levels by World Meteorological Organization (WMO). The Regional Specialized Meteorological Centres (RSMCs) and the Tropical Cyclone Warning Centres (TCWCs), listed in Tables A.1-2, have the regional responsibility to forecast and monitor each of the TC basins (Figure A.1). These centers provide information on TC position, intensity and other TC parameters, such as wind radii, on all TCs everywhere in the world. The RSMCs are responsible for tracking and issuing bulletins, warnings, and advisories about TCs in their designated areas of responsibility and additionally the TCWCs provide information to smaller regions. Also other organization, such as the Joint Typhoon Warning Center (JTWC), organizations provide information about tropical cyclones to the public (www.usno.navy.mil/JTWC).

RSMCs and TCWC archived also the TC best track data (BT), containing the best information available on TC position, intensity and other parameters obtained from observational and model data.

More information can be found on WMO web site and in Knaff et al. (2010).

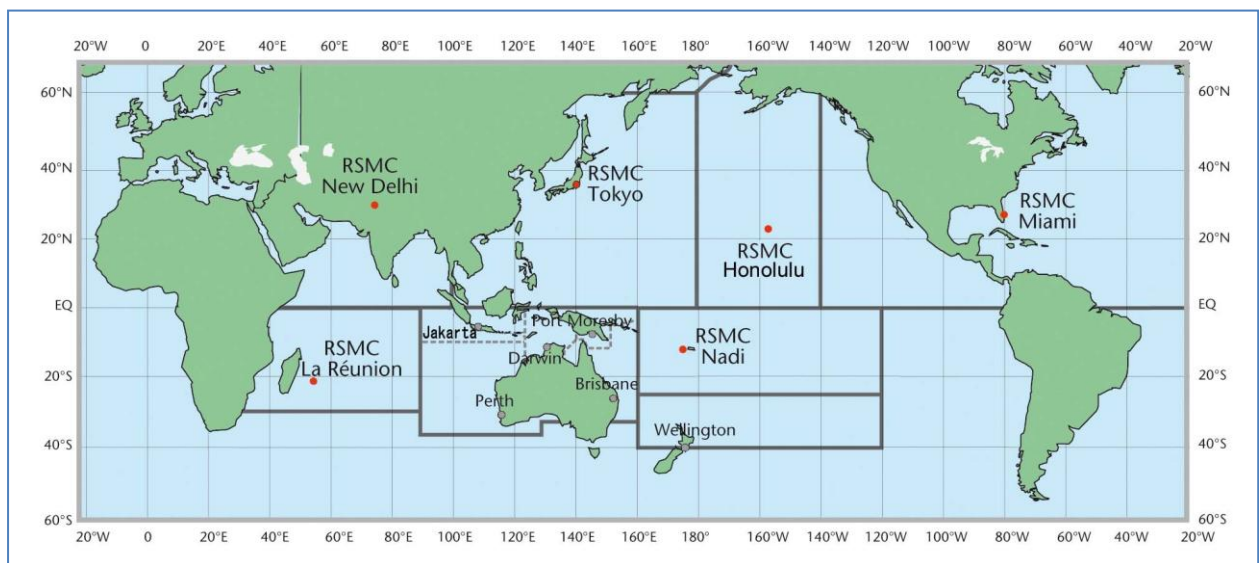


Figure A.1 – Map of the six Regional Specialized Meteorological Centres (RSMCs) and six Tropical Cyclone Warning Centres (TCWCs).

(Source: <http://www.wmo.int/pages/prog/www/tcp/Advisories-RSMCs.html>).

RSMC	ORGANIZATION	AREA
MIAMI-HURRICANE CENTER www.nhc.noaa.gov/index.shtml	NOAA/NWS National Hurricane Center, USA	Caribbean Sea Gulf of Mexico North Atlantic North Pacific Oceans
HONOLULU-HURRICANE CENTER www.prh.noaa.gov/hnl/cphc/	NOAA/NWS, USA	Central North Pacific Ocean
TOKYO-TYPHOON CENTER www.jma.go.jp/en/typh/	Japan Meteorological Agency	Western North Pacific Ocean South China Sea
TROPICAL CYCLONES NEW DELHI www.imd.gov.in	India Meteorological Department	Bay of Bengal Arabian Sea
LA RÉUNION - TROPICAL CYCLONE CENTRE www.meteo.fr/temps/dontom/La_Reunion/	Météo-France	South-West Indian Ocean
NADI-TROPICAL CYCLONE CENTRE www.met.gov.fj/advisories.html	Fiji Meteorological Service	South-West Pacific Ocean

Table A.1. – List of Regional Specialized Meteorological Centres (RSMCs).

TCWC	ORGANIZATION	AREA
PERTH www.bom.gov.au/weather/cyclone/	Bureau of Meteorology, Australia	South-East Indian Ocean
DARWIN www.bom.gov.au/weather/cyclone/	Bureau of Meteorology, Australia	Arafura Sea Gulf of Carpentaria
BRISBANE www.bom.gov.au/weather/cyclone/	Bureau of Meteorology, Australia	Coral Sea
PORT MORESBY <i>Website under construction</i>	National Weather Service, Papua New Guinea	Solomon Sea Gulf of Papua
WELLINGTON www.metservice.co.nz/forecasts/severe_weather.asp	Meteorological Service of New Zealand, Ltd.	Tasman Sea
JAKARTA www.bmg.go.id	Indonesian Meteorological and Geophysical Agency, Indonesia	Tasman Sea

Table A.2. – List of Tropical Cyclone Warning Centres (TCWCs).

APPENDIX B: Saffir-Simpson Scale

Category	Winds (1 min sustained winds)			
	knots	mph	km/h	m/s
HURRICANE 5	≥ 136	≥ 156	≥ 250	≥ 70
HURRICANE 4	114–135	131-155	210–249	59–69
HURRICANE 3	96–113	111-130	178–209	50–58
HURRICANE 2	83–95	96-110	154–177	43–49
HURRICANE 1	64–82	74-95	119–153	33–42
Tropical storm	35-64	39–73	63–117	18-32
Tropical depression	0-34	0–38	0–62	0-18

Table B.1 - Saffir-Simpson Scale

European Commission

EUR 25233 EN – Joint Research Centre – Institute for the Protection and Security of the Citizen
Title: Atmospheric forcing for a global storm surge forecast and inundation modeling
Authors: Pamela Probst, Giovanni Franchello

Luxembourg: Publications Office of the European Union
2012 – 47 pp. – 29.7 x 21 cm
EUR – Scientific and Technical Research series – ISSN 1831-9424
ISBN 978-92-79-23176-6
DOI 10.2788/14951

Abstract

Tropical cyclones (TCs) are some of the most damaging events. They occur in yearly cycles and affect the coastal population with three dangerous effects: heavy rain, strong wind and storm surge. In order to estimate the area and the population affected by a cyclone, all the three types of physical impacts must be taken into account. Storm surge is an abnormal rise of water above the astronomical tides, generated by strong winds and drop in the atmospheric pressure. The report describes the implementation of such phenomena in the JRC HyFlux2 code, which is routinely used in GDACS (www.gdacs.org) to model inundations due to tsunami run-ups.

The first aim of this work is to identify which source of information (provided by the different weather forecast centers) allows the specification of the pressure and wind fields of the TCs at global level. The lack of a global and free downloadable TC wind and pressure datasets has led the JRC to develop a Monte Carlo method to determine the Holland's parameters using the world available wind radii data (advisory and forecast). The obtained Holland's parameters are therefore used to obtain pressure and wind fields which are the forcing of the HyFlux2 storm surge modeling.

The developed methodology has been validated for four TCs: Earl, Nargis, Katrina and Yasi. The preliminary results show that it is possible to forecast the effects of storm surges by several days in advance.

How to obtain EU publications

Our priced publications are available from EU Bookshop (<http://bookshop.europa.eu>), where you can place an order with the sales agent of your choice.

The Publications Office has a worldwide network of sales agents. You can obtain their contact details by sending a fax to (352) 29 29-42758.

The mission of the JRC is to provide customer-driven scientific and technical support for the conception, development, implementation and monitoring of EU policies. As a service of the European Commission, the JRC functions as a reference centre of science and technology for the Union. Close to the policy-making process, it serves the common interest of the Member States, while being independent of special interests, whether private or national.



ISBN 978-92-79-23176-6



9 789279 231766